The middle Smithian (Early Triassic) ammonoid Arctoceras blomstrandi: conch morphology and ornamentation in relation to stratigraphy

Hansen, Bitten B. ; Bucher, Hugo ; Schneebeli-Hermann, Elke ; Hammer, Øyvind

Abstract: The ammonoid genus Arctoceras (Hyatt) occurs across all palaeolatitudes, and is a key genus for middle Smithian biostratigraphical correlations globally. In this study, intraspecific variations in conch morphology, ornamentation and allometry are examined in relation to stratigraphic position. Arctoceras is the most abundant ammonoid genus in the middle Smithian of Svalbard. Originally, seven Arctoceras species were described from Svalbard. Later, as the importance of intraspecific variation was recognized, six of the Arctoceras species from Svalbard were treated as junior synonyms of Arctoceras blomstrandi (Lindström). Yet, the variations in A. blomstrandi conch morphology remain poorly quantified and the dependence on stratigraphic position, unknown. We quantify the intraspecific variation in conch morphology, ornamentation and allometry in relation to stratigraphy of the Svalbard Arctoceras. The results support the assignment of all Arctoceras morphotypes from Svalbard to a single species A. blomstrandi. The new data allow for an updated species description and open the way for the use in biostratigraphy of the endmember morphology A. blomstrandi var. costatus. We document consistent changes in conch morphology and ornamentation in the studied stratigraphic interval, with a distinct shift towards more evolute and ornate conchs in the top of the interval. The trends in the strength of ornamentation are partly explained by covariation with conch morphology (Buckman's law). The most marked shift in the conch morphology and allometric development of A. blomstrandi coincides with the onset of the positive carbon isotope excursion at the end of the middle Smithian, but pre-dates the mid–late Smithian cooling of the sea surface.

DOI: https://doi.org/10.1002/spp2.1348

[Papers in Palaeontology, 2020, pp. 1–23]

THE MIDDLE SMITHIAN (EARLY TRIASSIC) AMMONOID *ARCTOCERAS BLOMSTRANDI*: CONCH MORPHOLOGY AND ORNAMENTATION IN RELATION TO STRATIGRAPHY

by BITTEN B. HANSEN[1], HUGO BUCHER[2], ELKE SCHNEEBELI-HERMANN[2] *and* ØYVIND HAMMER[1]

[1]Natural History Museum, University of Oslo, Pb. 1172 Blindern, 0318, Oslo, Norway; b.b.hansen@nhm.uio.no, oyvind.hammer@nhm.uio.no
[2]Paläontologisches Institut und Museum, Karl-Schmid-Strasse 4, 8006 Zürich, Switzerland; hugo.fr.bucher@pim.uzh.ch, elke.schneebeli@pim.uzh.ch

Typescript received 26 February 2020; accepted in revised form 6 October 2020

Abstract: The ammonoid genus *Arctoceras* (Hyatt) occurs across all palaeolatitudes, and is a key genus for middle Smithian biostratigraphical correlations globally. In this study, intraspecific variations in conch morphology, ornamentation and allometry are examined in relation to stratigraphic position. *Arctoceras* is the most abundant ammonoid genus in the middle Smithian of Svalbard. Originally, seven *Arctoceras* species were described from Svalbard. Later, as the importance of intraspecific variation was recognized, six of the *Arctoceras* species from Svalbard were treated as junior synonyms of *Arctoceras blomstrandi* (Lindström). Yet, the variations in *A. blomstrandi* conch morphology remain poorly quantified and the dependence on stratigraphic position, unknown. We quantify the intraspecific variation in conch morphology, ornamentation and allometry in relation to stratigraphy of the Svalbard *Arctoceras*. The results support the assignment of all *Arctoceras* morphotypes from Svalbard to a single species *A. blomstrandi*. The new data allow for an updated species description and open the way for the use in biostratigraphy of the endmember morphology *A. blomstrandi* var. *costatus*. We document consistent changes in conch morphology and ornamentation in the studied stratigraphic interval, with a distinct shift towards more evolute and ornate conchs in the top of the interval. The trends in the strength of ornamentation are partly explained by covariation with conch morphology (Buckman's law). The most marked shift in the conch morphology and allometric development of *A. blomstrandi* coincides with the onset of the positive carbon isotope excursion at the end of the middle Smithian, but pre-dates the mid–late Smithian cooling of the sea surface.

Key words: ammonoids, conch morphology, allometry, Buckman's law, Smithian, intraspecific variation.

EARLY Triassic ammonoids are of particular interest because they offer a detailed record of large-scale ecosystem recovery after the end-Permian mass extinction (Brayard *et al.* 2006; Ware *et al.* 2015). The magnitude and rate of this recovery are among the largest in the Phanerozoic. Understanding ammonoid evolution and dispersal in this critical phase requires detailed taxonomic work in order to provide accurate information on biodiversity, and on palaeobiogeographical, biostratigraphical and phylogenetic relationships. Within the Early Triassic, the Smithian–Spathian boundary is presently receiving a heightened interest. The boundary is marked by the final stage of the late Smithian extinction event of ammonoid and conodont species, which is connected to large-scale changes in climate and sealevel. A global upper Smithian hiatus has made the temporal extent of the event difficult to assess (Galfetti *et al.* 2007; Brayard & Bucher 2015; Widmann *et al.* 2020). The event signified the end of a diversification–extinction cycle that extended throughout the entire Smithian. The initial diversification phase took place during the early Smithian, with a high origination rate at the family level. The middle Smithian interval was marked by a thermal maximum (Romano *et al.* 2013; Goudemand *et al.* 2019), along with the appearance of short-lived ammonoid species in the Tethys Realm (Brühwiler *et al.* 2010, 2011). A widespread and stepwise extinction unfolded throughout the late Smithian (Brühwiler *et al.* 2010; Brayard & Bucher 2015; Jattiot *et al.* 2016), which brought Ammonoidea close to extinction. Moreover, a worldwide glacio-eustatic hiatus

doi: 10.1002/spp2.1348

spanned the Smithian–Spathian boundary (Hammer *et al.* 2019), the duration of which was quantified in South China by Widmann *et al.* (2020).

The Early Triassic ammonoids known from Svalbard were to a large extent described and named long ago (Lindström 1865; Mojsisovics 1886; Frebold 1930). A coherent regional stratigraphy was not developed until 1965 (Buchan *et al.* 1965), and prior to this, species were described from material collected with limited stratigraphic control, sometimes only referable to the formation level. Combined with a prevailing typological approach, the poor stratigraphic resolution obscured intraspecific and ontogenetic variation, which could consequently lead to taxonomic over-splitting. Over-splitting at the species level very likely leads to mistakes in biostratigraphic and palaeobiogeographic studies as well as to faulty interpretations of trends in phylogeny, evolution and diversity. Furthermore, palaeoecological analyses will be affected by the erroneous inflation of species richness. A typological approach to species definition evidently also leads to problems in the estimation of the effects of extinction and diversification events. This was, for instance, addressed by Jattiot *et al.* (2016) for the cosmopolitan genus *Anasibirites* at the late Smithian extinction, in which only two species out of 60 in the literature proved valid. Intraspecific variation in ammonoids can affect most morphological traits, but the most dramatic variations are found in the degree of compression/depression of the whorl section and in the degree of involution/evolution of the conch. As embodied in the so-called Buckman law of covariation (Buckman 1892, p. 313; Westermann 1966, p. 305; Hammer & Bucher 2005; Monnet *et al.* 2015), these coiling parameters tend to correlate with the strength of the ornamentation, with wide and evolute conchs usually being the most ornate. In addition, allometry (change in shape through growth) and variations in adult size can complicate the circumscription of sound morphological species.

In Svalbard, the genus *Arctoceras*, along with associated taxa, indicates strata of middle Smithian age. In terms of relative abundance, *Arctoceras* largely dominates the middle Smithian ammonoid fauna of Svalbard. Representatives of *Arctoceras* collected in Svalbard were originally assigned to seven species (as detailed below), until Kummel (1961) reassessed the type specimens in light of intraspecific variation. Based on the original material, Kummel concluded that all previously described species had overlapping characteristics and he regarded them as ontogenetic or morphological variants of one species, *Arctoceras blomstrandi* (Lindström, 1865). However, prior to the present study, *Arctoceras* was never collected bed by bed in Svalbard, and Kummel (1961) had no information with which to assess the intraspecific variation in relation to stratigraphic position. Therefore, a thorough revision based on new bedrock-controlled material is necessary to confidently determine which species of *Arctoceras* are present in Svalbard. Moreover, a reassessment of *Arctoceras* is an ideal case study to understand how morphological variants and/or species might vary throughout a middle Smithian succession.

For this study, we collected extensive material of *Arctoceras* from four sections in central Spitsbergen (Figs 1, 2) to document the morphological variation of the genus through geological time.

History of Arctoceras blomstrandi *in Svalbard*

Seven species of *Arctoceras* were recognized in Svalbard prior to the work by Kummel (1961): *A. blomstrandi* (Lindström, 1865); *A. costatus* (Öberg, 1877); *A. lindströmi* (Mojsisovics, 1886); *A. öbergi* (Mojsisovics, 1886); *A. polare* (Mojsisovics, 1886); *A. simplex* (Mojsisovics, 1886); and *A. whitei* (Mojsisovics, 1886).

Lindström, Öberg and Mojsisovics described their species under the genus *Ceratites*, which Diener (1915) later assigned to *Arctoceras* (Hyatt, 1900), with *Ceratites polaris* as the type species. Lindström worked on Svalbard ammonoids that had been collected by Nordenskjöld in 1864. Lindström described the new species *Ceratites? blomstrandi* in Latin (he found the lobes in the sutures to be inconclusive with regards to assigning genus). Lindström's specimens had been collected from 'shale and sandstone' at 'Midterhuken' and, as seen from his illustrations, they were highly damaged (Lindström 1865). Lindström's initial species description (Lindström 1865, p. 4) reads as follows, in English translation and with our interpretations in square brackets:

'Shell discoidal, compressed, involute, on both sides open and wide umbilicus, rounded back [venter]. Five windings. Outer winding large, embracing more than half of the internal ones; curved inwards sub-rectangularly [umbilical shoulder is angular]; surface gently folded [ribbed] transversely, folds [ribs] sigmoidal, almost as if the umbilicum is knotbearing [umbilical shoulder almost tubercular], covered with very thin furrows [striae]. Shell of the back longitudinally striated [conch bears ventral strigation]. Lateral saddles (only two visible) regularly arcuate, lobes faintly dentate. Shell diameter 77 mm. Outer winding is 28 mm high, 16 mm wide, widest in the middle [chamber is widest halfway between umbilical shoulder and venter].'

Öberg undertook fieldwork in Svalbard in 1872 as part of an expedition focused on geological resources (Öberg 1877). The expedition collected in localities on Midterhuk, building upon the material collected by Nordenskjöld in 1864. Öberg (1877) also included material collected on another polar expedition in 1868 and

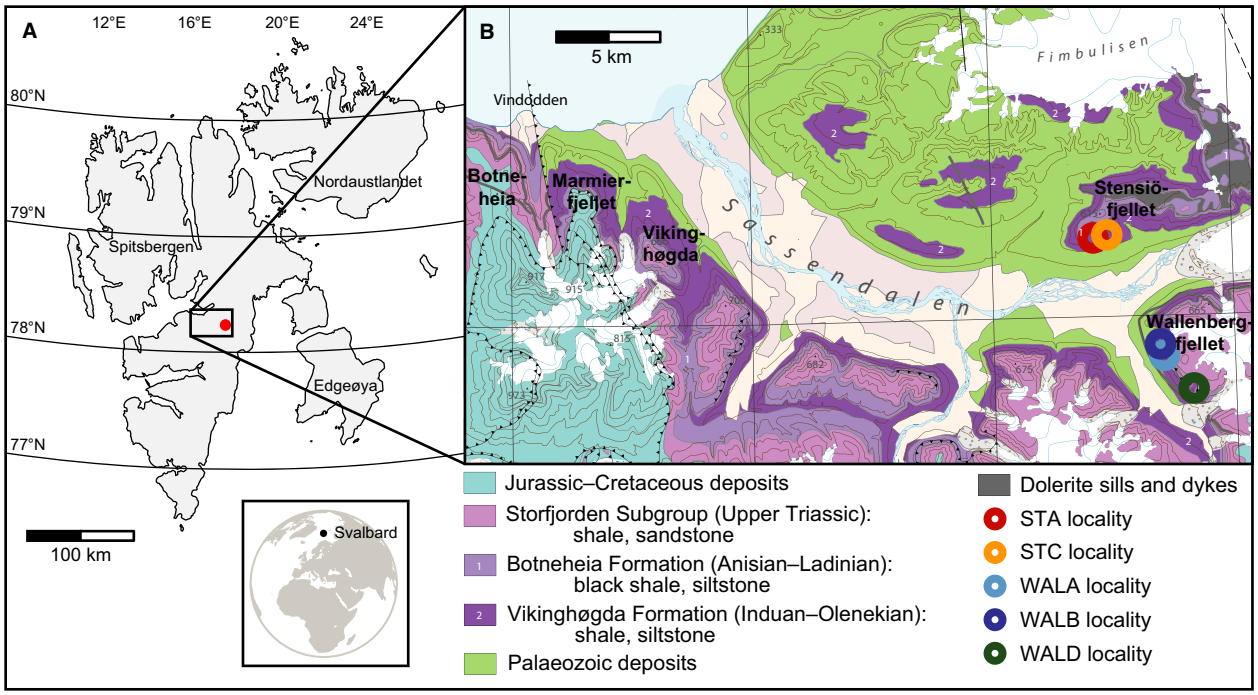

FIG. 1. Map of Svalbard with the 2017 field area marked. A, location of the studied sections in central Spitsbergen. B, geological map of the Sassendalen area. The five studied sections: STA, 78°17′02.8″N; 017°42′20.1″E; STC, 78°16′59.8″N; 017°44′22.5″E; WALA, 78°14′03.6″N; 017°50′53.4″E; WALB, 78°14′19.7″N; 017°50′21.1″E and WALD, 78°13′12.5″N; 017°54′42.7″E. Lithologies are redrawn from a geological map of Svalbard (Major *et al.* 2001).

material collected by Nathorst in 1870. Öberg had material of fair preservation and he confirmed the species *Ceratites blomstrandi* as suggested by Lindström (1865). Öberg described the largest specimens in his collection as being largely like Lindström's *C. blomstrandi* but having true nodes/tubercles on the umbilical shoulder. The nodes would often turn into ribs on the lateral shell, he observed, and these did not cross the venter. The material came from calcareous concretions in 'the marly shale' at 'Svarta Klyfta' (Öberg 1877). According to Buchan *et al.* (1965), 'Svarta Klyften' (or 'Klyfta' in Swedish) is a section at Kapp Thordson (Kapp Thordsen on the southern tip of Dickson Land; Norwegian Polar Institute 2003), and likewise is the 'Isfjord-Kolonie' of Mojsisovics (1886) and 'Midterhuk' of Lindström (1865). This locates all the original material in the same area of central Spitsbergen, north of Isfjorden. Öberg (1877) went on to describe the new species *Ceratites costatus* based on a single individual found in 1872 at Svarta Klyfta. *C. costatus* largely resembles *C. blomstrandi* but has notable differences. *C. costatus* is described as having a comparatively rounded umbilical shoulder with no tubercles, although Öberg suggested that they might develop at an older stage. The ribs are strong and straighter than in *C. blomstrandi*, and on the outer whorls they cross the venter, forming convex arcs. Near the aperture, the venter appears slightly 'bumpy' between the ribs when viewed laterally. According to Öberg (1877), the suture lines of *C. blomstrandi* and *C. costatus* are very similar, although *C. costatus* is supposed to have two umbilical lobes, as opposed to the one of *C. blomstrandi*.

In 1886, Mojsisovics reassessed the *Arctoceras* material of Lindström and Öberg and established five new species: *A. lindströmi*, *A. öbergi*, *A. polare*, *A. simplex* and *A. whitei*. The five species were based on few and generally poorly preserved specimens, making the suggested differences highly questionable. Furthermore, the splitting done by Mojsisovics is a typical example of the confusing of ontogenetic changes with species-specific traits.

In 1961, Kummel reviewed the earlier described material and provided new reliable illustrations of the holotypes and paratypes in order to compare actual differences and similarities of the fossils. Kummel (1961, fig. 1) included a diagram of the measured characteristics of more than 200 Spitsbergen *Arctoceras* specimens from the collection in the British Museum (Natural History), including the holotypes of the existing species. The diagram plots the chamber height (*wh*) and umbilical diameter (*uw*) against the conch diameter (*d*) of each specimen. All specimens fall within a general trend with no distinct groupings and, lacking the relevant stratigraphic data, Kummel concluded that only one *Arctoceras* species is

present in Svalbard, and that it has a randomly variable conch.

After collecting *Arctoceras* in Svalbard across multiple sections, it became clear that the variation in the genus is not random with respect to stratigraphy. Individuals collected from the lower part of a section are always large and ribbed, individuals from around the middle always small, compressed and generally lacking ornamentation, and towards the top of a section the individuals again become slightly larger, less compressed and more strongly ornamented. In this work we re-evaluate Kummel's single *Arctoceras* species in Svalbard to test its robustness.

GEOLOGICAL SETTING

Strata of Early Triassic age in Svalbard are represented by the Vardebukta and Tvillingodden formations on the west coast of Spitsbergen and by the Vikinghøgda Formation in the central and eastern parts of the archipelago. The Vikinghøgda Formation was deposited on an offshore shelf and represents the distal equivalent of the coastal to shallow marine Vardebukta and Tvillingodden formations (Mørk *et al.* 1999; Wignall *et al.* 2016). The Vikinghøgda Formation consists of three members: the Deltadalen Member was deposited during the Griesbachian and Dienerian, the Lusitaniadalen Member was deposited during the Smithian, and the Vendomdalen Member during the Spathian. The two latter members correspond to the Tvillingodden Formation in the west. The Lusitaniadalen and Vendomdalen members are relatively fossil-rich and fairly well-defined in terms of biostratigraphy (Buchan *et al.* 1965; Mørk *et al.* 1999; Hammer *et al.* 2019).

The lithological boundary between the Lusitaniadalen and Vendomdalen members more or less coincides with the boundary between the Smithian and Spathian substages. However, there is probably a hiatus spanning the latest Smithian, and the substage boundary is included in this gap (Hammer *et al.* 2019). In the Lusitaniadalen Member, the only preserved late Smithian zone is the early late Smithian *Wasatchites tardus* Zone (British Columbia, Tozer 1994; northern Siberia, Dagys 1994). In the low latitudes, the late Smithian ammonoid biostratigraphy includes at least two zones (North Indian Margin, Brühwiler *et al.* 2010; Western USA Basin, Jattiot *et al.* 2017), only the oldest of which is correlated in the high latitudes (Hammer *et al.* 2019). Therefore, as stressed by Hammer *et al.* (2019), the youngest part of the late Smithian is typically missing in the Boreal Realm, indicating a hiatus. In the Lusitaniadalen Member, rocks yielding middle Smithian ammonoids are directly overlain by rocks representing the early late Smithian *Wasatchites tardus* Zone. The entire succession of strata with middle Smithian ammonoids (dominated by *Arctoceras*) has in Svalbard traditionally been assigned to a single zone, namely the *Euflemingites romunderi* Zone. However, the type species is in fact absent from the lower part of the section and only the upper part is assuredly within the *E. romunderi* Zone (Weitschat & Dagys 1989; Mørk *et al.* 1999). No older Smithian zones have been confirmed in the Lusitaniadalen Member.

Throughout the Boreal Realm, *A. blomstrandi* occurs in association with middle Smithian taxa (Korchinskaya 1972; Weitschat & Dagys 1989; Dagys & Ermakova 1990; Tozer 1994). Only in two cases are *A. blomstrandi* possibly associated with younger strata. From Ellesmere Island (Arctic Canada) in a single locality, Tozer (1994) described an association of *A. blomstrandi* with species of the late Smithian *W. tardus* Zone. Tozer himself questioned the authenticity of this assemblage of middle and late Smithian taxa that could have resulted from either condensation or reworking. The other case is the unconfirmed association of *Arctoceras erebori* (which we synonymize with *A. blomstrandi*) with xenoceltids and prionitids of the *W. tardus* Zone from Stensiöfjellet (Piazza *et al.* 2017). The ammonoids were in this case all extracted from a large concretion of which the internal structure and stratigraphy is unknown.

MATERIAL AND METHOD

We collected extensive ammonoid material along with sediment samples for organic carbon analysis in Sassendalen (central Spitsbergen, Svalbard) from two sections at Stensiöfjellet (STA and STC) and three sections at Wallenbergfjellet (WALA, WALB and WALD) (Fig. 1). In Stensiöfjellet, the two sections were reasonably close to each other and had similar developments, and they were measured and sampled as one. In Wallenbergfjellet, the sections were more distant and were logged separately. Fossils were not brought back from the distant WALD section, but it is included here because of its significance in biozone correlation. Lithological log, macrofossil contents and organic carbon isotopes from each section are shown in Figure 2.

Lithology, fossil occurrences and biozonation

The level datum (0 m) used for the logs (Fig. 2), corresponds to the boundary between the Lusitaniadalen and Vendomdalen members. In Wallenbergfjellet, the boundary is consistent with the definition by Mørk *et al.* (1999) and is found on the upper surface of a yellow-weathering, silty bed. The bed is part of the grey shales of the Lusitaniadalen Member and the top of the bed corresponds to

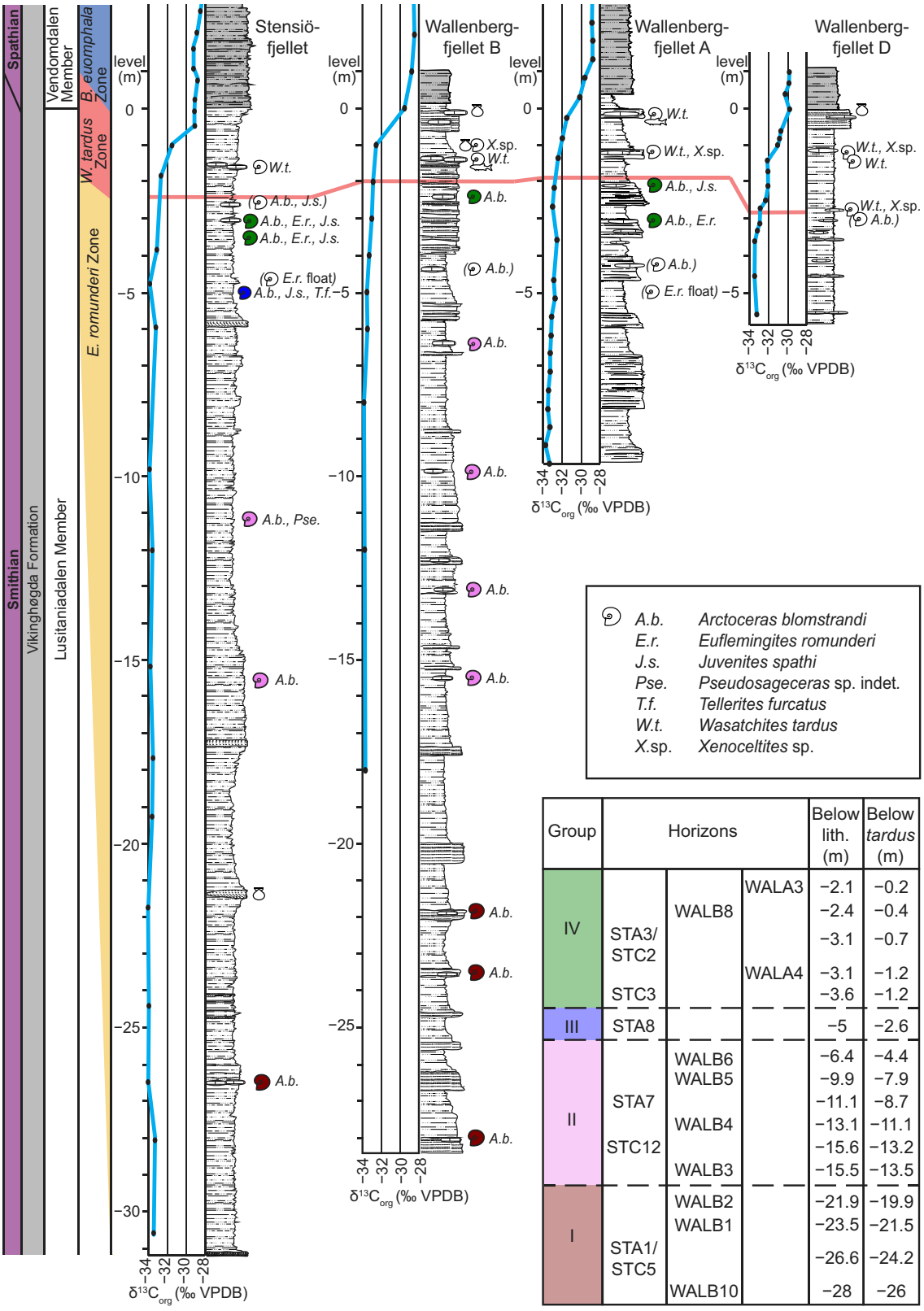

Group	Horizons			Below lith. (m)	Below *tardus* (m)
IV	STA3/STC2	WALB8	WALA3	−2.1	−0.2
				−2.4	−0.4
				−3.1	−0.7
			WALA4	−3.1	−1.2
	STC3			−3.6	−1.2
III	STA8			−5	−2.6
II	STA7	WALB6		−6.4	−4.4
		WALB5		−9.9	−7.9
				−11.1	−8.7
	STC12	WALB4		−13.1	−11.1
				−15.6	−13.2
		WALB3		−15.5	−13.5
I	STA1/STC5	WALB2		−21.9	−19.9
		WALB1		−23.5	−21.5
				−26.6	−24.2
		WALB10		−28	−26

FIG. 2. Lithostratigraphic logs showing the investigated sections and corresponding $\delta^{13}C_{org}$ logs from Sassendalen. The attempted correlation of the lower limits of the *W. tardus* Zone across sections is based on fossil finds in combination with $\delta^{13}C_{org}$ values. Inserted table gives the composition of the four stratigraphic groups to which the horizons are assigned for analysis.

the approximate base of the Spathian (Mørk *et al.* 1999; Hammer *et al.* 2019). At Stensiöfjellet, the yellow-weathering silty bed appeared to be missing and an abrupt change from grey to black shales is used as the member boundary. Further field work by one of us (HB) in 2020 confirmed that the boundary bed is actually present at Stensiöfjellet, although it was not exposed in 2017. All the studied sections can be expected to have highly similar lithological developments. Selective preservation is obvious in the Lusitaniadalen Member in all sections, given that ammonoids are found only within early diagenetic carbonaceous lenticular horizons and nodules. The surrounding shales almost exclusively yield flattened bivalves, if anything at all.

The lowermost *Arctoceras* specimens were sampled at −28 m (section WALB) in relation to the Lusitaniadalen–Vendomdalen boundary, while the highest sample was located at −2.1 m (section WALA) (Fig. 2). We confirmed *Wasatchites tardus*, demonstrating the early late Smithian *W. tardus* Zone at different heights in the separate sections. The upper boundary of the *W. tardus* Zone is uncertain, but it is probably located slightly above the lithological boundary (Hammer *et al.* 2019). The uppermost *W. tardus* specimen was sampled in section WALA at *c.* −0.1 m, while the lowermost was sampled in section WALD at −2.7 m. In all sections there is a minor gap between *in situ* fossils of the *E. romunderi* Zone and the *W. tardus* Zone, but in section WALD that gap is as little as 0.3 m, with *Arctoceras* found at −3 m.

The vertical extent of the *W. tardus* Zone is difficult to define precisely because it is relatively thin, and may be demonstrated from as little as only one nodular horizon in a section. An attempt to use the organic carbon isotope curves to aid correlation between sections is shown in Figure 2. The WALD section has the longest proven extent of the *W. tardus* Zone, with three observations spanning 1.6 m. The gap between the lowest *W. tardus* and the highest *Arctoceras* specimen (demonstrating the *E. romunderi* Zone) is also thinner here than in the other sections. The gap has a $\delta^{13}C_{org}$ value of −33‰ VPDB (Vienna Pee Dee Belemnite standard). This value is traced across all studied sections as a tentative correlation of the interval separating the *E. romunderi* and *W. tardus* Zones (Fig. 2). The suggested $\delta^{13}C_{org}$ correlation line falls close to the uppermost *Arctoceras* samples in each section, and might indicate that these are in fact of similar age, despite differences in lithological development between sections. However, care is taken in ordering samples from separate sections in relation to each other, and for the following analyses, the sampled *Arctoceras* horizons are treated as belonging to one of four stratigraphic groups: Group I, II, III or IV (Figs 2–6). The number of stratigraphic groups was set to minimize the risk of incorrect correlations and to obtain sufficient sample sizes for statistical analysis.

Arctoceras were collected in association with the following ammonoid species (Fig. 2).

Euflemingites romunderi (Tozer, 1961): *in situ* specimens of *E. romunderi* (Fig. 6I) were found only between −3.1 and −3.6 m (horizons STA3, WALA4 and STC3).

Juvenites spathi (Frebold, 1930): *J. spathi* (following the definition of Jattiot *et al.* 2017) (Fig. 6H) was found between −2.1 and −5 m (horizons WALA3, STA3, STC2, STC3 and STA8).

Tellerites furcatus (Öberg, 1877): several specimens of *T. furcatus* (Fig. 5H, I) were found at −5 m (horizon STA8). The species was placed exclusively in the *Wasatchites tardus* Zone by Weitschat & Dagys (1989), but we have been able to confirm it only in a single horizon in the *Euflemingites romunderi* Zone.

Pseudosageceras sp. indet. (Diener, 1895): a single *Pseudosageceras* specimen was found in association with *Arctoceras* at −11.1 m (horizon STA7). The genus has earlier been observed only in the *W. tardus* Zone (Weitschat & Dagys 1989; Mørk *et al.* 1999). Given that *Pseudosageceras* is a long-raging genus, the variable age occurrence is not unexpected.

Fossil data

The material collected for this work consists of 135 *Arctoceras* specimens (of which seven specimens are measured twice at different growth stages) from 18 horizons (Figs 2, 7). Levels where *Arctoceras* specimens were present but not collected are shown in parentheses in Figure 2. Sample sizes from the different horizons are highly dissimilar, and 12 horizons are represented by five or fewer sets of measurements. The material is curated at the Paläontologisches Institut und Museum, Universität Zürich, Switzerland, and figured specimens have received catalogue numbers of this institution (PIMUZ). *Arctoceras* specimens were measured and described following Klug *et al.* (2015). For each specimen, measurements were taken for the largest preserved diameter *d* and corresponding whorl width *ww*, whorl height *wh* and umbilical width *uw*. When the conch was not complete on both sides, the half width was measured on the intact side and the full whorl width inferred. All measurements are available in the Dryad Digital Repository (Hansen *et al.* 2020). In some damaged specimens the best measurements were obtained not on the outermost whorl, but on a younger part of the conch (measurements noted with a '*' in the online dataset; Hansen *et al.* 2020). Specimens with diameters

FIG. 3. *Arctoceras blomstrandi* specimens of Group I. Star indicates last suture when visible. A, PIMUZ37610 (STC5, −26.6 m; *uw/d*, 0.17; *ww/d*, 0.25); B, PIMUZ37593 (STA1, −26.6 m; *uw/d*, 0.30; *ww/ d*, 0.29); C, PIMUZ37612 (WALB2, −21.9 m; *uw/d*, 0.26; *ww/d*, 0.29). Scale bars represent 10 mm.

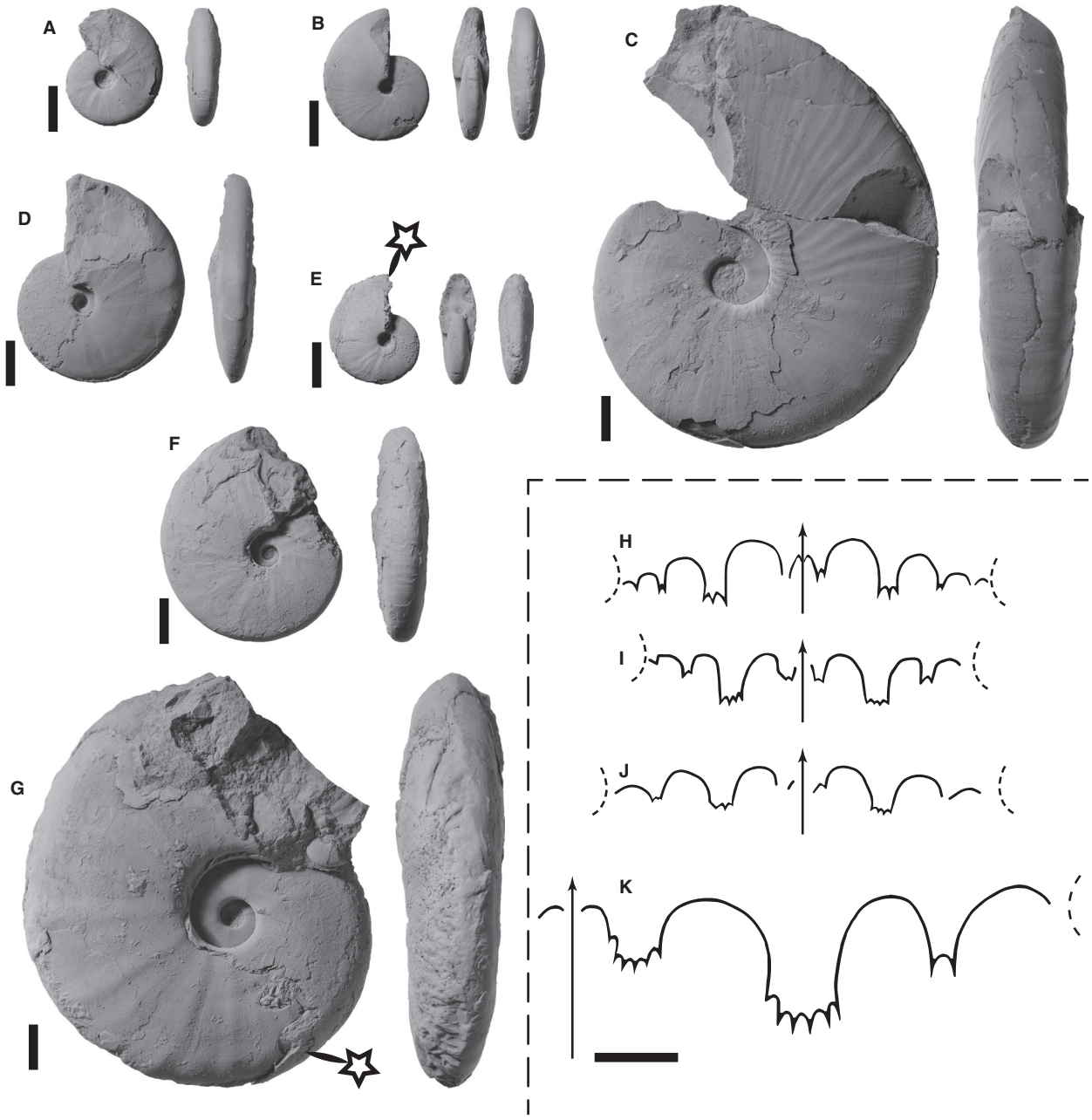

FIG. 4. *Arctoceras blomstrandi* specimens of Group II and suture lines sampled from groups I, III and IV. Star indicates last suture when visible. A, PIMUZ37613 (WALB5, −9.9 m; *uw/d*, 0.14; *ww/d*, 0.28); B, PIMUZ37615 (WALB5, −9.9 m; *uw/d*, 0.11; *ww/d*, 0.30); C, PIMUZ37614 (WALB5, −9.9 m; *uw/d*, 0.18; *ww/d*, 0.28); D, PIMUZ37602 (STC12, −15.6 m; *uw/d*, 0.12; *ww/d*, 0.26); E, PIMUZ37604 (STC12, −15.6 m; *uw/d*, 0.12; *ww/d*, 0.34); F, PIMUZ37603 (STC12, −15.6 m; *uw/d*, 0.16; *ww/d*, 0.29); G, PIMUZ37601 (STC12, −15.6 m; *uw/d*, 0.19; *ww/d*, 0.30); H, PIMUZ37616 suture at d = ~43 mm (WALB8, −2.4 m); I, PIMUZ37600 suture at d = ~37? mm (STA8, −5 m); J, PIMUZ37596 suture at d = 45? mm (STA8, −5 m); K, PIMUZ37593 suture at d = ~200 mm (STA1, −26.6 m). Scale bars represent 10 mm.

below *c.* 10 mm were not included in analyses because of the low measuring accuracy. Qualitative characterization of shell ornamentation (i.e. ribs) is also considered for each specimen (weak/strong/absent). When a specimen was too damaged, the ornamentation was characterized as 'unknown' (Hansen *et al.* 2020). Data processing was done using the free software PAST, version 3.24 (Hammer *et al.* 2001).

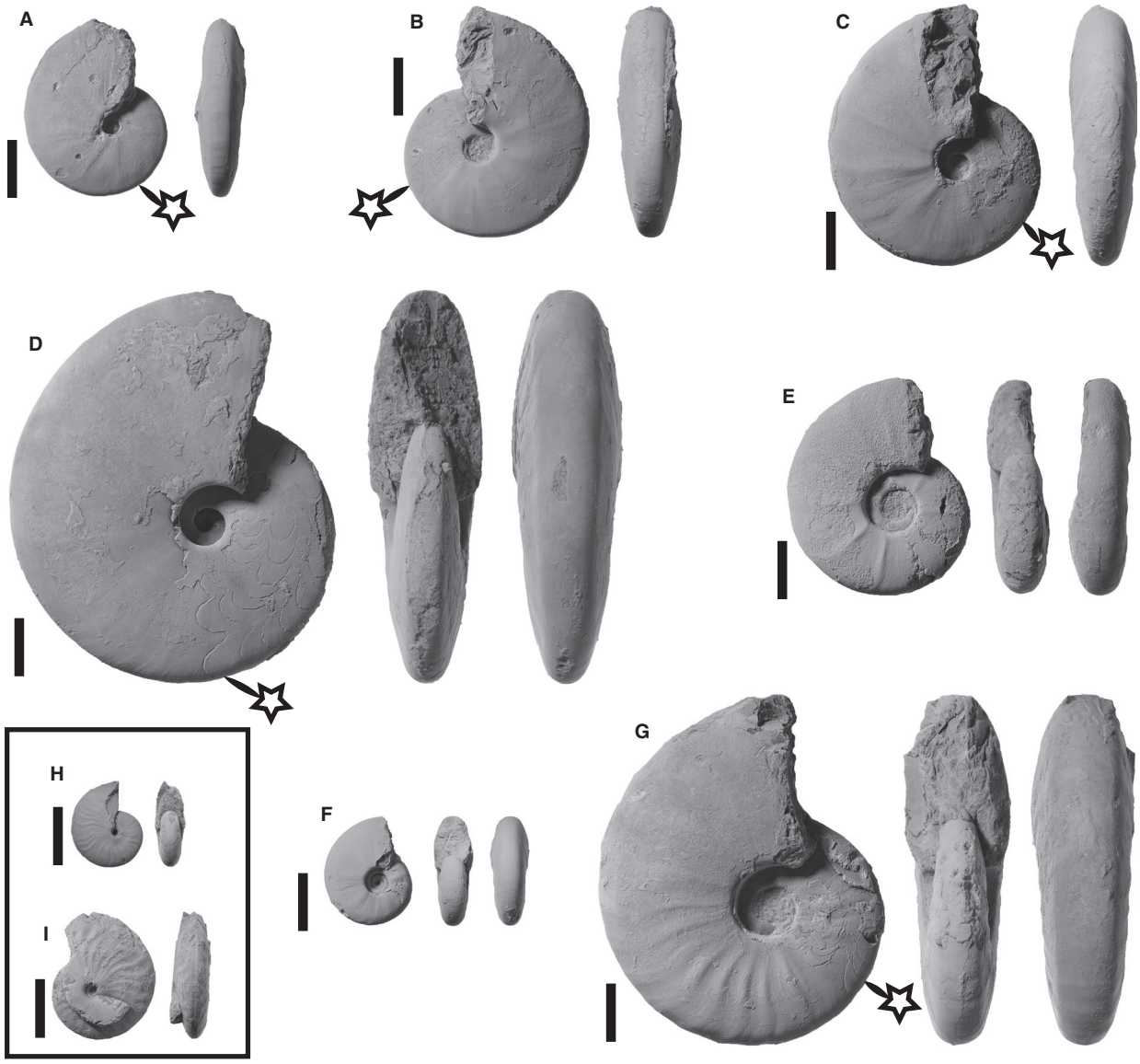

FIG. 5. *Arctoceras blomstrandi* specimens of Group III along with examples of associate fauna sampled from a single float block at *c.* −5 m below the top of the Lusitaniadalen Member (STA8). Star indicates last suture when visible. A, PIMUZ37598 (*uw/d*, 0.12; *ww/d*, 0.31); B, PIMUZ37597 (*uw/d*, 0.17; *ww/d*, 0.33); C, PIMUZ37595 (*uw/d*, 0.16; *ww/d*, 0.27); D, PIMUZ37596 (*uw/d*, 0.16; *ww/d*, 0.28); E, PIMUZ37594 (*uw/d*, 0.28; *ww/d*, 0.32); F, PIMUZ37599 (*uw/d*, 0.24l *ww/d*, 0.36); G, PIMUZ37600 (*uw/d*, 0.21; *ww/d*, 0.30); H, PIMUZ37621, *Tellerites furcatus*; I, PIMUZ37620, *Tellerites furcatus.* Scale bars represent 10 mm.

$\delta^{13}C_{org}$ logs

The $\delta^{13}C_{org}$ curve from the WALB section shown in Figure 2 originates from Hammer *et al.* (2019). The $\delta^{13}C_{org}$ curves from the Stensiöfjellet, WALA and WALD sections were prepared at the Paläontologisches Institut und Museum, Universität Zürich, Switzerland and measured at the University of Lausanne, Switzerland. Fifty-five samples were selected for bulk organic carbon isotope composition ($\delta^{13}C_{org}$); all pulverized using a ceramic mortar. About 5 g of powdered samples were dissolved in 6 M hydrochloric acid to remove all carbonates. After centrifuging, residues were rinsed several times with deionized water and centrifuged until neutrality was reached. The residues were dried overnight at 45°C, and $\delta^{13}C_{org}$ values of the homogenized residues were measured using a Carlo Erba 1500 elemental analyser connected to a ThermoFisher Delta V Plus mass spectrometer at the University of Lausanne. The samples were individually wrapped in tin foil cups and sequentially allowed to react

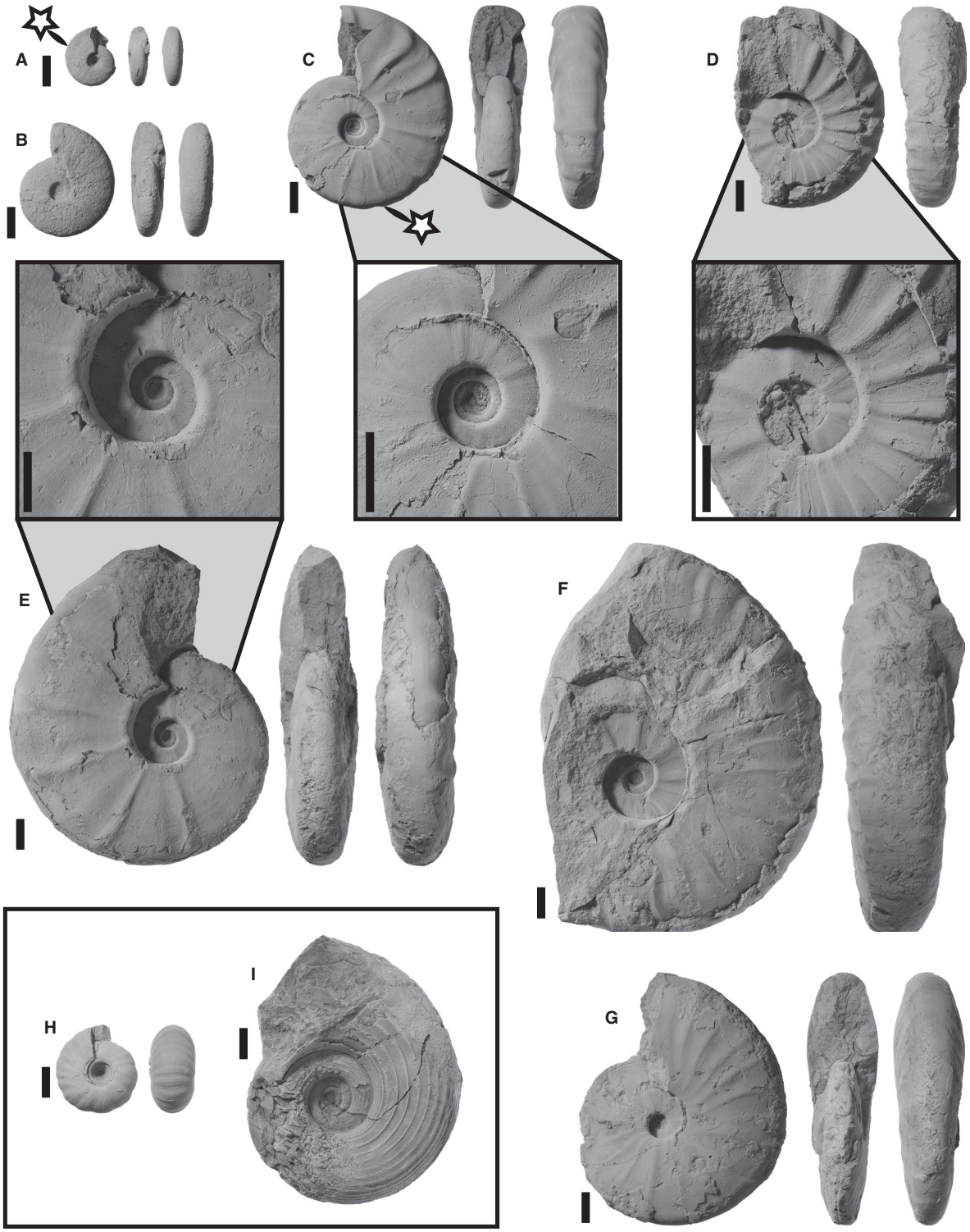

FIG. 6. *Arctoceras blomstrandi* specimens of Group IV along with examples of associate species. Star indicates last suture when visible. A, PIMUZ37611 (WALA3, −2.1 m; *uw/d*, 0.26; *ww/d*, 0.36); B, PIMUZ37606 (STC2, −3.1 m; *uw/d*, 0.22; *ww/d*, 0.34); C, PIMUZ37616 (WALB8, −2.4 m; *uw/d*, 0.24; *ww/d*, 0.29); D, PIMUZ37609 (STC3, −3.6 m; *uw/d*, 0.28; *ww/d*, 0.36); E, PIMUZ37592 (STA3, −3.1 m; *uw/d*, 0.22; *ww/d*, 0.35); F, PIMUZ37607 (STC2, −3.1 m; *uw/d*, 0.26; *ww/d*, 0.34); G, PIMUZ37608 (STC3, −3.6 m; *uw/d*, 0.18; *ww/d*, 0.28); H, PIMUZ37622, *Juvenites spathi* (WALA3, −2.1 m); I, PIMUZ37623, *Euflemingites romunderi* (STA3, −3.1 m). Scale bars represent 10 mm.

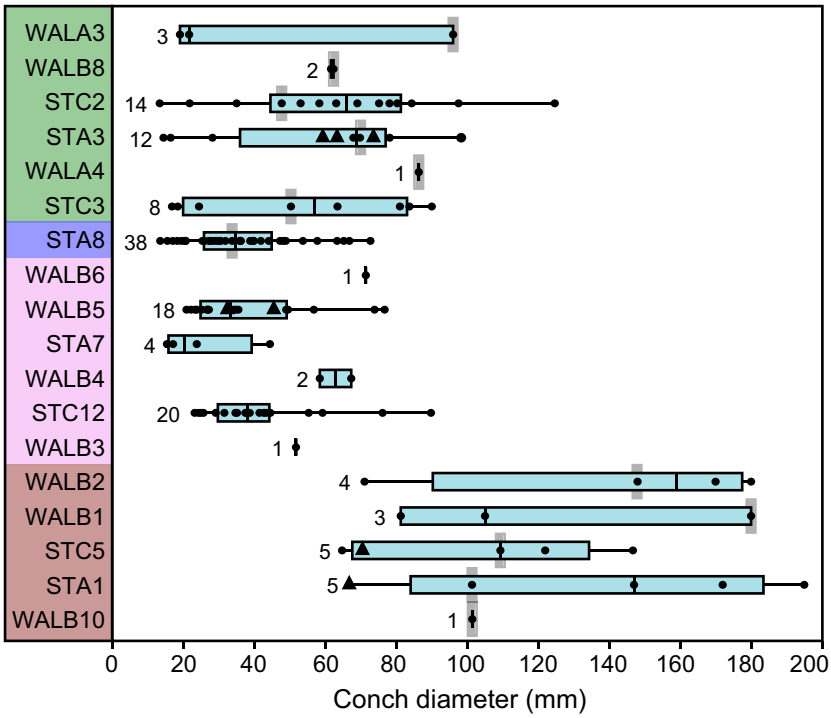

FIG. 7. Box and dot plot showing the size (diameter) distribution of specimens within the sampled horizons (sorted according to stratigraphic group). Boxes extend from the 25th to the 75th percentiles, with the median shown as a vertical line within the box. Solid triangular data points signify internal data from a larger specimen. The number of data points in each horizon is noted at the left of the boxes. Grey shading signifies the smallest known specimen with strong ribs within a horizon.

with an injected quantity of oxygen while continuously flushed with He carrier gas. The sample was oxidized in the reactor at *c.* 1050°C using cobalt(II) oxide as the catalyst. Excess oxygen in the He-stream was adsorbed in a reactor column filled with metallic Cu held at 500°C. The CO_2 produced was passed over a magnesium perchlorate ($Mg[ClO_4]_2$) trap to remove H_2O, and a gas chromatograph to separate the N_2 from the CO_2, before the CO_2 was carried by the He-stream into the mass spectrometer for isotopic analysis. The reproducibility of several in-house standards used is better than 0.1‰, and they are calibrated against USGS-24 graphite (−16.0‰ VPDB).

RESULTS

Size and maturity

Figure 7 shows a box and dot plot of the measured conch diameters within each horizon. The median value (shown as a vertical line) is given in each box. An obvious change in specimen size is observed from the lower to the middle part of the section between the samples of horizon WALB2 (−21.9 m) and of WALB3 (−15.5 m). Although the basal horizons (Group I, −28 m to −21.9 m) contain no specimens smaller than 64 mm in diameter, the rest of the section (−15.5 to −2.1 m) is dominated by small specimens <100 mm. Only a single complete specimen from horizon STC2 reaches a diameter of 125 mm. In some horizons (STC12, WALB4, STC2 and WALA3), scattered fragments of large individuals (with an inferred diameter of more than 100 mm; Hansen *et al.* 2020) indicate that the observed size trend is in part due to preservation bias. The preserved conch sizes in the lower (Group I, −28 to −21.9 m) and upper (Group IV, −3.6 to −2.1 m) horizons appear fairly symmetrically distributed. Conversely, the size distribution of the horizons in between (Group II, −15.6 to −6.4 m; Group III, −5 m) is markedly skewed, with many relatively small specimens and a right tail of larger specimens. This distribution pattern could be interpreted as a higher juvenile mortality in the palaeoenvironment of these horizons. Another interpretation could be that the individuals of these horizons have mechanically lost most of their flattened body chambers during extraction in field and therefore appear smaller, overall. Unfortunately, the material is rarely preserved with sutures and there is not much direct evidence for or against the two interpretations. The general absence of sutures likewise makes it difficult to assess at what diameter *Arctoceras* reached maturity. Generally, in specimens in which the sutures are visible, the body chamber is at least partially preserved, showing that the entire phragmocone at the time of death can be expected to be preserved across the material (Figs 3–6). Septal crowding at the end of the phragmocone, which is diagnostic of maturity, is rarely observed in the material. From horizon WALB2 at −21.9 m a poorly preserved

specimen (PIMUZ37612; Fig. 3C) shows crowding of both ribs and sutures. The specimen was at least 170 mm in total diameter and the last suture sits at a diameter of *c.* 125 mm. From the upper part of the section at −3.1 m (STC2), a very poorly preserved fragmental specimen (PIMUZ37605) appears to have approximated ribs towards the venter. The fragment originates from an individual with a diameter of at least 150 mm. The sutures are, however, not preserved in PIMUZ37605. These two specimens might indicate that the maximum size of *Arctoceras* is constant or near-constant across the stratigraphy, but to thoroughly assess the question of size and maturity, more and better material will be needed.

Ornamentation

Ornamentation, mainly in the form of relatively distant lateral ribs, as a rule stronger on outer whorls, is unevenly distributed through stratigraphy. The notion of whether ribs are strong or weak is qualitative and somewhat arbitrary. However, distinctly strong ribs are dominant in the lower horizons (Group I, −28 to −21.9 m), where specimens are large. In the middle part of the section (Group II, −15.6 to −6.4 m), all specimens lack strong ribs except for a single fragmental large individual (inferred original diameter of 100–125 mm) at −13.1 m (WALB4). In the upper part of the section (Groups III and IV, −5 to −2.1 m), strong ribs are present even though specimens are not generally larger than in the middle part. Ribbing in *Arctoceras* has a highly flexible nature and usually appears very gradually through growth. Figures 3–6 show selected specimens from the four stratigraphic groups.

Conch morphology in relation to stratigraphy

Figure 8 shows scatterplots of the individual measured coiling parameters of all specimens and demonstrate how the four stratigraphic groups cluster in morphospace. Figure 8A shows the umbilical width index (*uw/d*) versus the diameter of all specimens. Large specimens of Group I (−28 to −21.9 m) appear to form a linear trend, consistent with the smaller specimens from Groups II (−15.6 to −6.4 m) and III (−5 m), and describe a widening umbilicus in relation to diameter with age/size. Specimens of Group IV (−3.6 to −2.1 m) have overlap with the other groups, but many individuals plot in the far upper left part of the morphospace (i.e. they are more evolute than any other specimens of similar size). The specimens from Group III (−5 m) have a large spread in umbilical width indexes, but appear to form an intermediate cluster between Groups II and IV, with which they have a large overlap.

Figure 8B shows whorl height normalized to diameter (*wh/d*) versus diameter. As could be expected, the distribution is similar to that of Figure 8A, but vertically inverted, and whorl height decreases in relation to diameter with age/size (involute specimens have relatively large values for *wh/d*).

Figure 8C–D demonstrates two different, but closely related, expressions of conch shape (Fig. 8C: *ww/d*, conch width index; Fig. 8D: *ww/wh*, whorl width index). A similar trend is seen in the two plots: specimens from Group I form a cluster mostly separate from the rest of the material. Groups II and III are unable to be separated and also overlap largely with Group IV. Group IV does, however, spread far into the upper part of the morphospace, having wider conchs and whorl sections than other specimens at similar diameters.

The morphological parameters of the stratigraphic groups can also be expressed in two dimensions, as in the box plots in Figure 9. Figure 9A (*uw/d*) shows a peculiar signal (reversed in Fig. 9B for *wh/d*): Group I has large values, but the immediately overlaying Group II has comparably small values. Through Groups II to IV, the values increase again to a level comparable to that of Group I. Using the descriptive terms from Klug *et al.* (2015), individuals of Groups I and IV are nearly all subinvolute (*uw/d*, 0.15–0.30), while Groups II and III tend heavily towards involute conchs (*uw/d*, <0.15).

When considering the conch width (*ww/d*) and whorl width (*ww/wh*) indices (Fig. 9C, D), there is a slight, but unmistakable, increase in values from Groups I to IV. However, the size bias between the stratigraphic groups is severe (Fig. 7), and the relationship between size and conch morphology (ontogentic development) is investigated further below.

Isometry/allometry of umbilical width in relation to stratigraphy

The degree of conch evolution appears to be ontogenetically controlled, given that the umbilical width index (uw/d) generally increases with size across the dataset (Fig. 8A). We study this ontogenetic pattern using nonlinear regression of umbilical width against conch diameter for the allometric equation $y = ax^b$ (i.e. forcing a zero intercept), with bootstrapped confidence intervals. We chose this method over the classical log-log transformation (which would yield a linear regression) because it gives a more direct and easily interpretable picture of the ontogenetic development (de Queiroz 1998). The regression coefficients for the allometric equation are given in

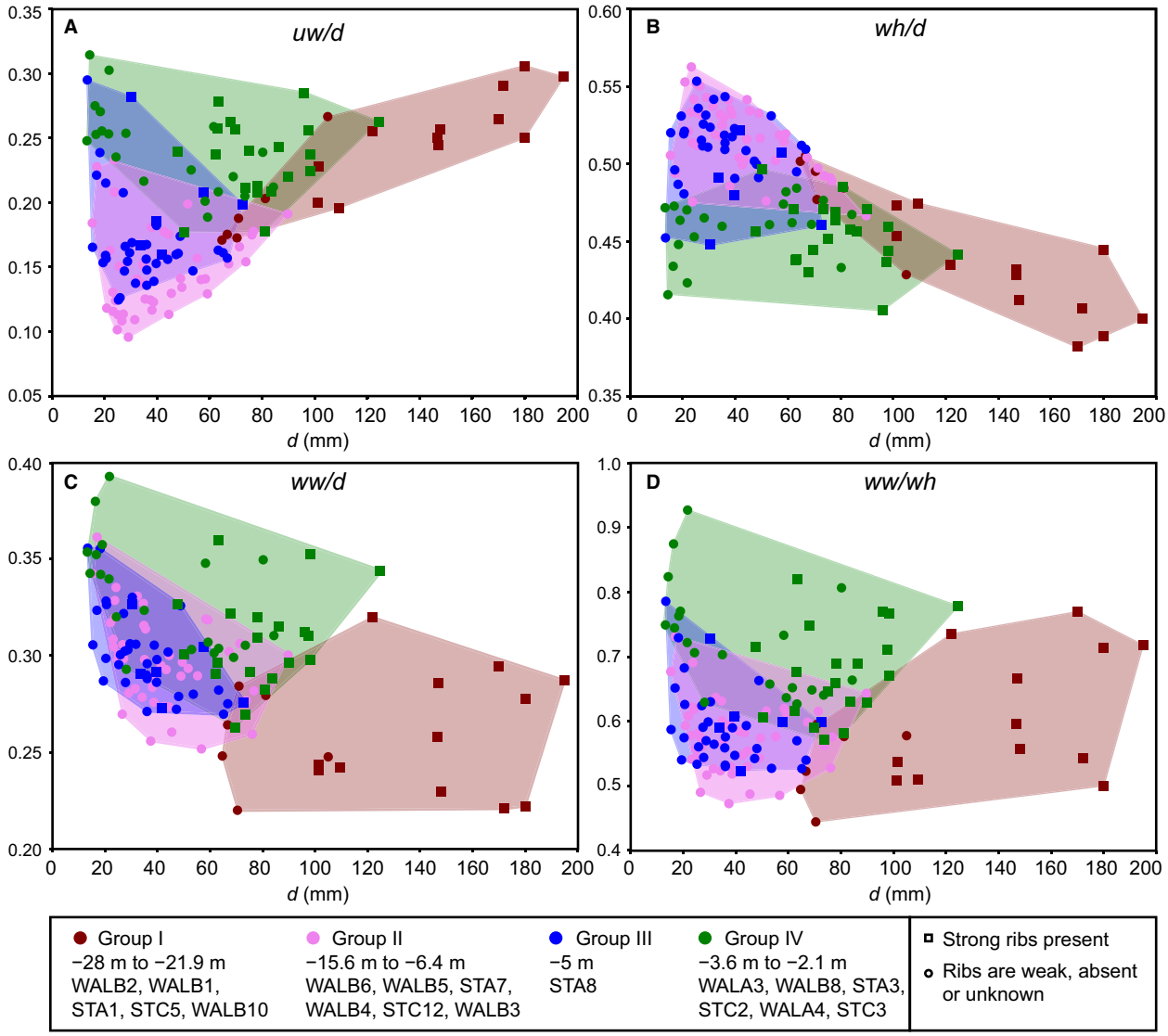

FIG. 8. Scatterplots of conch shape ratios. Specimen colours correspond to stratigraphic grouping. A, Umbilical width index *uw/d*. B, Whorl height index *wh/d*. C, Conch width index *ww/d*. D, Whorl width index *ww/wh*.

Table 1 and the resulting allometric curves are shown in Figure 10A.

There is a considerable reduction in the allometric coefficient *b* from Group I at the bottom of the section up to Group III at −5 m, describing a shift from allometry to sub-isometry in the ontogenetic development of uw. Although the 95% confidence intervals are overlapping between adjacent groups, there is no overlap between Groups I and III, and the trend is reliable (Fig. 10A, inset). Sub-isometry is also seen for Group IV at the top. An immediate problem with the data is the severe size bias between groups. In Group III the growth pattern beyond d = ~70 mm is uncertain, and *uw* might actually have a more allometric development than can be proven from the recovered material. The sub-isometric growth in Group IV is more well-founded and reliable. At the same time as the allometric coefficient is shown to decrease upsection, the scaling coefficient *a* increases from 0.03 at the bottom of the section up to 0.17 at the top. The trends in coefficients *a* and *b* lead to a complex relationship between size, degree of evolution (*uw/d*) and stratigraphy. At small sizes (d < 60 mm), the overall conch evolution undisputedly increases from the lower levels to the top of the section (Fig. 10A). At intermediate sizes (d = 60–130 mm), the trend becomes obscured, but the most evolute conchs are still found at the top of the section (Group IV). At large conch sizes (d > 130 mm), Group I from the bottom of the section overtakes the other groups due to the strong positive allometry of this group. We are now able to explain the peculiar trend seen

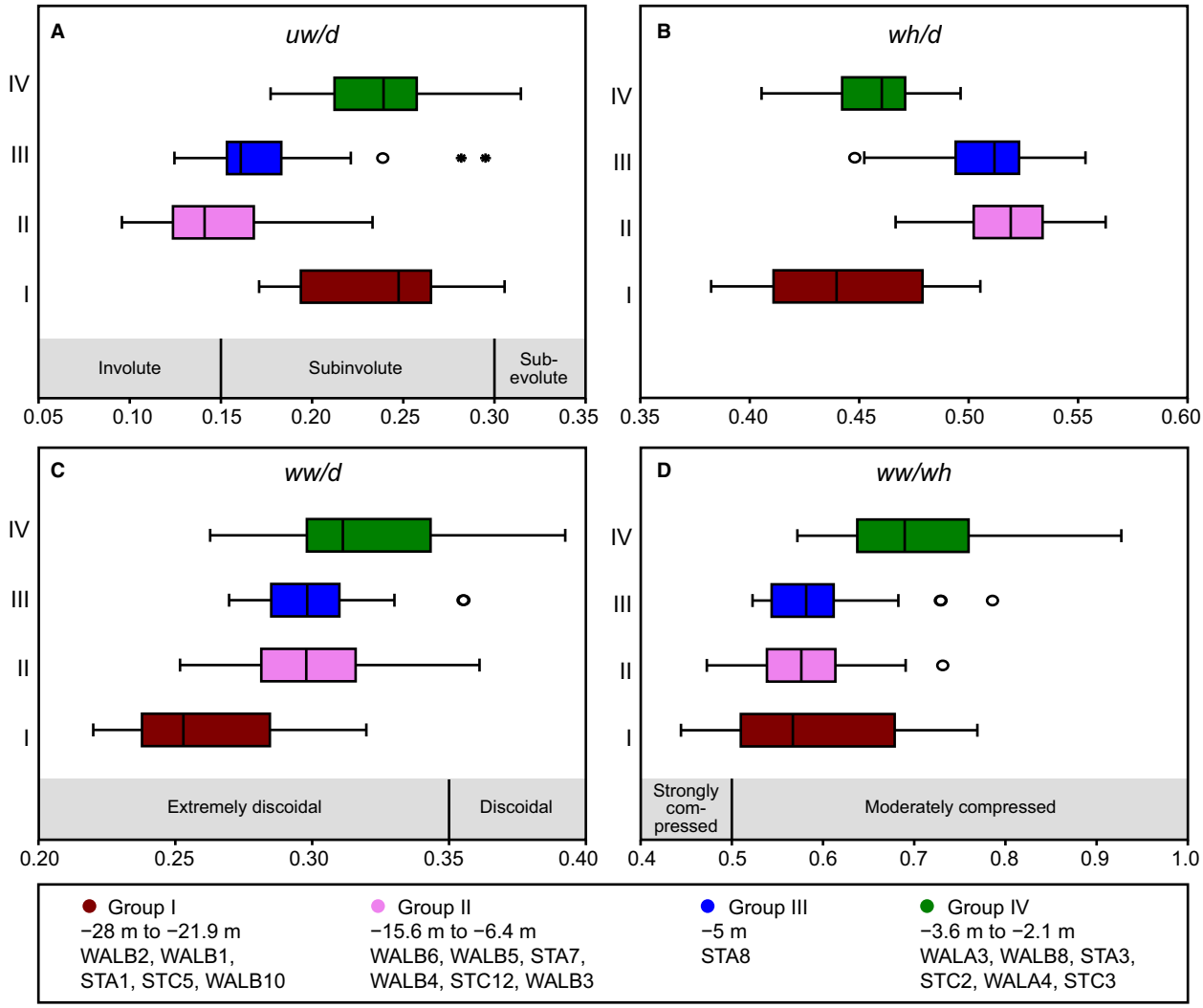

FIG. 9. Box plots showing the range of conch shape ratios in the four stratigraphic groups. Boxes extend from the 25th to the 75th percentiles, with the median shown as a vertical line within the box and outliers marked with symbols. Descriptive terms and definitions are based on Klug *et al.* (2015). A, umbilical width index *uw/d*. B, whorl height index *wh/d*. C, conch width index *ww/d*. D, whorl width index *ww/wh*.

TABLE 1. Regression coefficients for the allometric equation for umbilical width *uw* as a function of conch diameter *d*.

Group	Level (m)	*n*	*a*	*b*	95% CI on *b*
I	−28 to −21.9	18	0.03	1.45	1.32–1.60
II	−15.6 to −6.4	46	0.06	1.23	1.12–1.40
III	−5	38	0.16	1.02	0.85–1.21
IV	−3.6 to −2.1	40	0.17	1.07	0.95–1.23

in Figure 9A: given that only intermediate and large specimens were recovered in stratigraphic Group I, this group is represented solely by comparably evolute forms (relative large *uw/d* ratio). Groups II and III appear less evolute than Group I, mainly because only smaller conchs were recovered. Conversely, the relatively more evolute signal in Group IV is not an artefact of size, but an actual morphological development towards larger umbilical widths in the juvenile and sub-adult conchs.

Isometry of whorl width in relation to stratigraphy

We investigate the trends of whorl width (*ww*) against conch diameter (*d*) as a function of stratigraphic position, as was done for umbilical width above. The regression coefficients for the allometric equation are given in Table 2 and the resulting allometric curves are shown in Figure 10B.

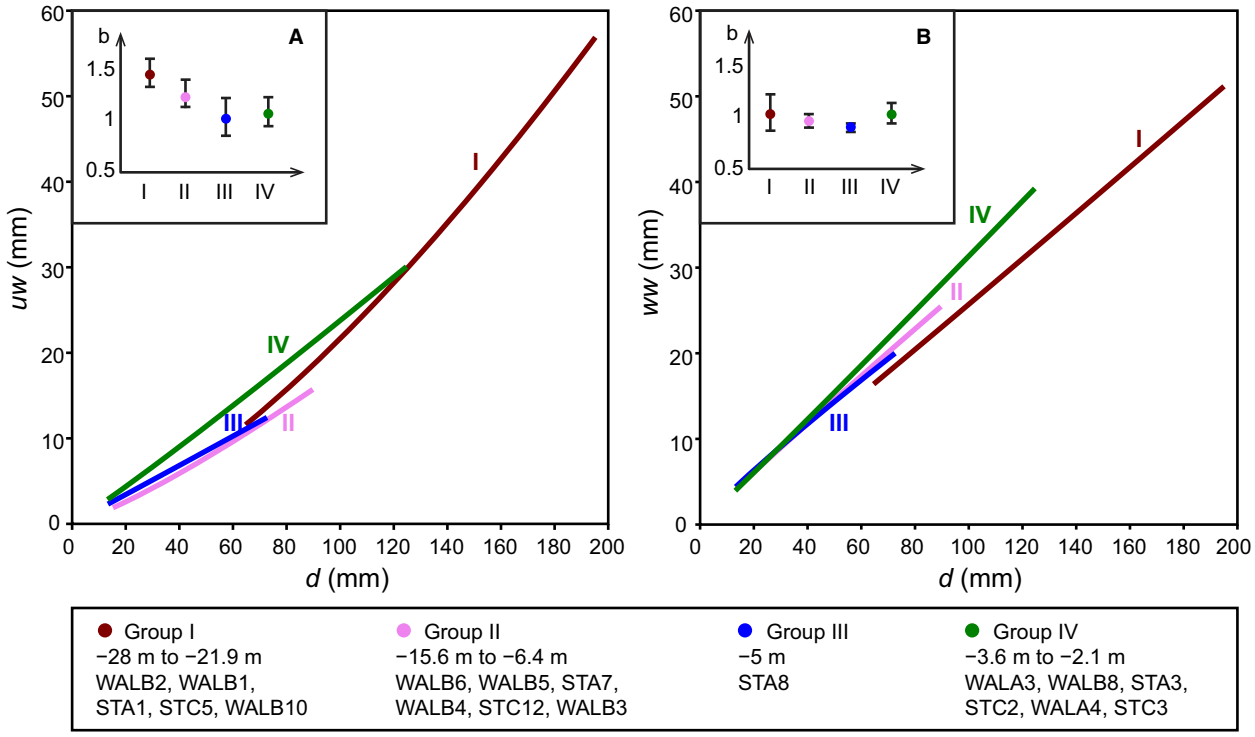

FIG. 10. Non-linear fits to the allometric equation $y = ax^b$. Inserted are b values with 95% confidence intervals. A, umbilical width *uw*. B, whorl width *ww*.

The allometric coefficients (Fig. 10B) are not significantly different from isometry ($b = 1$) except in Group III at −5 m, where a slight negative allometry is indicated. However, there is a stratigraphic trend, given that Group I from the bottom of the section exhibits the smallest whorl widths across all conch sizes. Meanwhile, Group IV from the top has the largest whorl widths for all conchs larger than 50–60 mm in diameter. Figure 9C depicted very much the same trend, which is now proven largely independent of the size bias. In Figure 9D, Groups I–III all have similar median values of *ww/wh*, in spite of the large differences in conch sizes within these levels. Group IV is the only stratigraphic group with a markedly different median value, indicating that a shift in conch morphology is taking place at the top of the section between Groups III and IV.

TABLE 2. Regression coefficients for the allometric equation for whorl width *ww* as a function of conch diameter *d*.

Group	Level (m)	*n*	*a*	*b*	95% CI on *b*
I	−28 to −21.9	18	0.22	1.03	0.88–1.21
II	−15.6 to −6.4	46	0.35	0.96	0.90–1.02
III	−5	38	0.43	0.90	0.86–0.93
IV	−3.6 to −2.1	40	0.28	1.02	0.93–1.14

Ornamentation and conch morphology: Buckman's law of covariation

Buckman's first law of covariation (Buckman 1892, p. 313; Westermann 1966, p. 305; Monnet *et al.* 2015; Moulton *et al.* 2015) states that more evolute and depressed individuals within a species tend to have coarser ornamentation. A simple explanation for this common phenomenon in terms of isometric scaling was given by Hammer & Bucher (2005). For testing Buckman's law of covariation in our material, we correlated strength of ribbing with *uw/d* (describing the degree of evolution) and *ww/wh* (describing the degree of compression) across the complete dataset. Strength of ribbing in each specimen was assessed qualitatively and assigned to three classes: absent, weak, and strong. Specimens with unknown ornamentation (due to surface damage) were not included and the total number of data points in the analysis is $N = 126$. A specimen can easily have weak or absent ribbing on the inner whorls followed by strong ribbing on the outer whorls (but not the other way around). Only the strongest degree of ribbing is noted. The strength of ribbing is, in the analysis, considered as an ordinal value reflecting an underlying continuous distribution, while *uw/d* and *ww/wh* are continuous variables. When testing the degree of ribbing versus *ww/wh*, we obtained $r = 0.18$, $p = 0.036$ (Spearman's rank-order correlation). This

means that the correlation is weak but statistically significant. For the ribbing versus *uw/d*, we obtained $r = 0.48$, $p < 0.001$. This is a fairly strong correlation that is highly significant. The specimens with absent or weak ribs ($n = 88$) are found to have a mean *uw/d* of 0.17 ± 0.01 (95% CI for the estimate of the mean). The specimens with strong ribs ($n = 38$) have a considerably higher mean *uw/d* of 0.24 ± 0.01 ($p < 0.001$, Mann–Whitney test).

The relatively strong correlation between the degree of evolution and ornamentation ($r = 0.48$) is in accordance with Buckman's law, and this can be at least partly invoked as responsible for the strong ornamentation of the stratigraphic groups I and IV, in which the observed degree of evolution is strongest (Fig. 9A).

$\delta^{13}C_{org}$ logs

Trends in bulk organic carbon isotope values from STA, WALA, and WALD are closely comparable. In all three sections, $\delta^{13}C_{org}$ from the lower part of the studied middle Smithian Lusitaniadalen Member ranges between *c.* −34‰ and *c.* −33‰ (Fig. 2). The onset of a slight positive trend is observed at STA, *c.* 5 m below the Lusitaniadalen–Vendomdalen boundary; the positive shift is distinctly expressed from 2 m below the boundary and continues until *c.* −29‰ is reached. At WALA, $\delta^{13}C_{org}$ shows a more gradual positive shift from −33.34‰ at the base to −28.79‰ at the top of the studied section (Fig. 2). At WALD, $\delta^{13}C_{org}$ in the lowest part of the studied succession is *c.* −33.5‰. It starts to increase 3.5 m below the Lusitaniadalen–Vendomdalen boundary and reaches *c.* −30‰ in the lowermost part of the Vendomdalen Member. In all three successions, preliminary observations (ESH) indicate that particulate organic matter does not significantly change in composition throughout the studied intervals. Thus, a compositional change in organic matter is unlikely to be the driving mechanism for the observed changes in bulk organic carbon isotopes values (Tyson 1995).

DISCUSSION

We have investigated the morphology, ornamentation and allometry of *Arctoceras* in Svalbard across stratigraphy. The taxon shows a large variation in conch parameters within each stratigraphic group, along with notable differences between groups. Even so, we consider the material as belonging to one species, *A. blomstrandi*. The overlap between adjacent stratigraphic groups is generally large and none of the groups can be completely separated from the bulk of the material, therefore the erection of two or more distinct species is not justified. Buckman's law of covariation can be shown to be partly responsible for the variation seen in the Svalbard arctoceratids, and no mode of ornamentation is decoupled from the main trend of the material. We still document a clear stratigraphic trend in *A. blomstrandi*, which is discussed and quantified further here.

Conch morphology, ornamentation and allometry in relation to stratigraphy

We have shown above how the bias in preserved conch size across stratigraphy is not the only controlling factor on the recovered conch morphologies in *A. blomstrandi*. There are undisputable differences in the ontogenetic development between the bottom and top of the section. The degree of conch evolution is the trait creating the most prominent variation in *A. blomstrandi* because this is also linked to the strength of ribbing (Buckman's law of covariation). When considering the ontogenetic development in umbilical width, a shift happens between Groups II and III from allometry to isometry (Fig. 10A). This means that in most of the section (−28 to −6.4 m), *uw/d* can be expected to increase during ontogeny, giving a slight un-coiling effect of the conch, a trait common in arctoceratids. Conversely, in the upper part of the section (−5 to −2.1 m), the umbilical width will tend to remain near constant in relation to the diameter throughout growth. From Group III to IV, further changes take place as the initial width of the umbilicus in relation to diameter increases. This is also seen from Figure 8A. When considering the ontogenetic development of the whorl width no shift is seen in the type of growth, given that all groups grow isometrically. However, the trend of larger relative sizes in the top of the section is seen here as well. Considering the trend in whorl section shape (*ww/wh*, Fig. 9D), the morphological shift is restricted to Group IV. When it comes to the development of ornamentation in *Arctoceras blomstrandi*, there are some uncertainties due to poor preservation and size biases. We have indications that in Groups I and II, strong ribs do not appear in small conchs ($d < 100$ mm) (Fig. 7). Conversely, in Groups III and IV, examples of very small individuals with prominent ribbing are known (e.g. PIMUZ37594; Fig. 5E). We showed that Buckman's law of covariation is in effect, and that the emergence of strong ribbing in small conchs is related especially to the widening of the umbilicus. The morphological changes in the conch of *Arctoceras blomstrandi* are strongest in Group IV, but appear to be initiated within Group III. Group III is in fact a single horizon, and the onset of morphological change is very well-defined at *c.* −5 m below the lithostratigraphic boundary.

Definition of a 'new' morphological endmember

It is the variations in conch coiling and ribbing that create the largest differences in appearance in *A. blomstrandi*. The earlier distinction between seven species in Svalbard was beyond doubt a gross exaggeration of the importance of each trait. However, given that we have shown that *A. blomstrandi* undergoes directional changes to its morphology through time, the question arises whether one species is in fact sufficient to cover the variation.

Kummel (1961, fig. 1) presented a plot of whorl height (*wh*) and umbilical diameter (= *uw*) against the conch diameter of Spitsbergen *A. blomstrandi* specimens in the collection at the British Museum (Natural History). As Kummel pointed out, all specimens fall within the same general trend and do not form obvious groupings. However, it is interesting to note how the holotype of *A. costatus* falls slightly outside the main plot with a relatively large umbilical width, as is the trend in *A. blomstrandi* towards the top of the stratigraphy. The *A. costatus* description was also the most distinct of the species descriptions following the initial description of *A. blomstrandi* by Lindström (Kummel 1961). In the present material we observe a number of *costatus*-like specimens that are in fact all found towards the top of the sections. However, although a specimen such as PIMUZ37616 (WALB8, d = 62.28 mm; Fig. 6C) is practically identical to the description by Öberg (1877) (see 'History of *Arctoceras blomstrandi*' above), there are some immediate problems with the *costatus* species description. In PIMUZ37592 (STA3, d = 98.23 mm; Fig. 6E), the ribs are distant and distinct but do not cross the venter, and the umbilical shoulder is not rounded. Rather, the umbilical shoulder is raised and it could even be argued that it is developing very faint tubercles towards the aperture. In PIMUZ37609 (STC3, d = 63.39 mm; Fig. 6D) the ribs cross the venter but the umbilical shoulder is again distinct and slightly raised, not rounded. The overall impression of *costatus* sets it apart from the bulk of *Arctoceras* specimens but the distinction between morphotypes is a difficult one to draw. This also means that the exact stratigraphic distribution of the *costatus* morphotype is uncertain. All the distinct specimens in our material are found in stratigraphic Group IV between −2.1 and −3.6 m. In Figure 11, we have plotted measurements of the holotype, paratype and lectotype specimens of the original *Arctoceras* species alongside the present material. Conch measurements are taken from Kummel (1961), Lindström (1865) and Mojsisovics (1886). Due to the poor preservation of the type material and differences in measuring standards, the given values are not entirely trustworthy; also, not all characteristics could be measured (hence, the uneven number of measurements included in the plots in Fig. 11). Still, all data points fit reasonably within the same trends as are described in this study, supporting the conclusion of a single species as drawn by Kummel (1961). In Figure 11A–B, the holotype of *costatus* plots neatly in the same areas as specimens sampled from the upper levels of the stratigraphy.

According to Öberg (1877), the suture line of *costatus* bears two umbilical lobes, as opposed to one in *A. blomstrandi*. Kummel (1961) was not able to confirm any consistent differences between suture lines of the various *Arctoceras* morphotypes in Svalbard, and even points to the fact that the suture line might vary on opposing sides of the same individual. In the present material, suture lines are not generally preserved, and the question has been difficult to study in full detail. In Figure 4H the suture line of the *costatus*-like specimen PIMUZ37616 is shown, and the two umbilical lobes are indeed present. However, the same appears to be the case in, for example, PIMUZ37596, a slim un-ornamented specimen, although the suture line proved difficult to draw at the umbilicus in all specimens (compare Figs 4J and 5D).

Here, we refrain from elevating the *costatus* morphotype to species level based on the generally high flexibility of the *Arctoceras* conch morphologies and the large overlap of morphologies across stratigraphic groups. Still, the *costatus* morphotype is a distinct endmember restricted to the top of the section, which makes it potentially useful in biostratigraphy. More *costatus* material from Svalbard and other Boreal localities might push our understanding of this particular morphotype, but currently there is no strong support for reinstating *costatus* as a separate species. For future biochronological descriptions and discussions, the endmember could be referred to as *A. blomstrandi* var. *costatus*.

Conch size in relation to stratigraphy

A substantial reduction in average conch size occurs in *Arctoceras blomstrandi* between Groups I and II from the sample at −21.9 m to the sample at −15.6 m. The associated changes in morphology (reduced degree of evolution and strength of ribbing) between these horizons are explained by the allometric effects of the size reduction. The reduction in observed sizes could be a preservation artefact, but may alternatively reflect changes happening in the palaeoenvironment. Perhaps an unstable environment led to increased juvenile mortality, seen as the deposition of an unproportionate number of many small conchs. Alternatively, the habitats of age groups switched, and juveniles became the dominant inhabitants of the area.

In Groups III and IV, the overall recovered conch size does not change substantially from Group II, but 'mature' morphology and ornamentation are developed at smaller sizes than previously, and the endmember morphology *A. blomstrandi* var. *costatus* may be observed. The lack of evidence of full maturity (in the form of approximating sutures and/or ribs) would suggest that *A. blomstrandi* at the

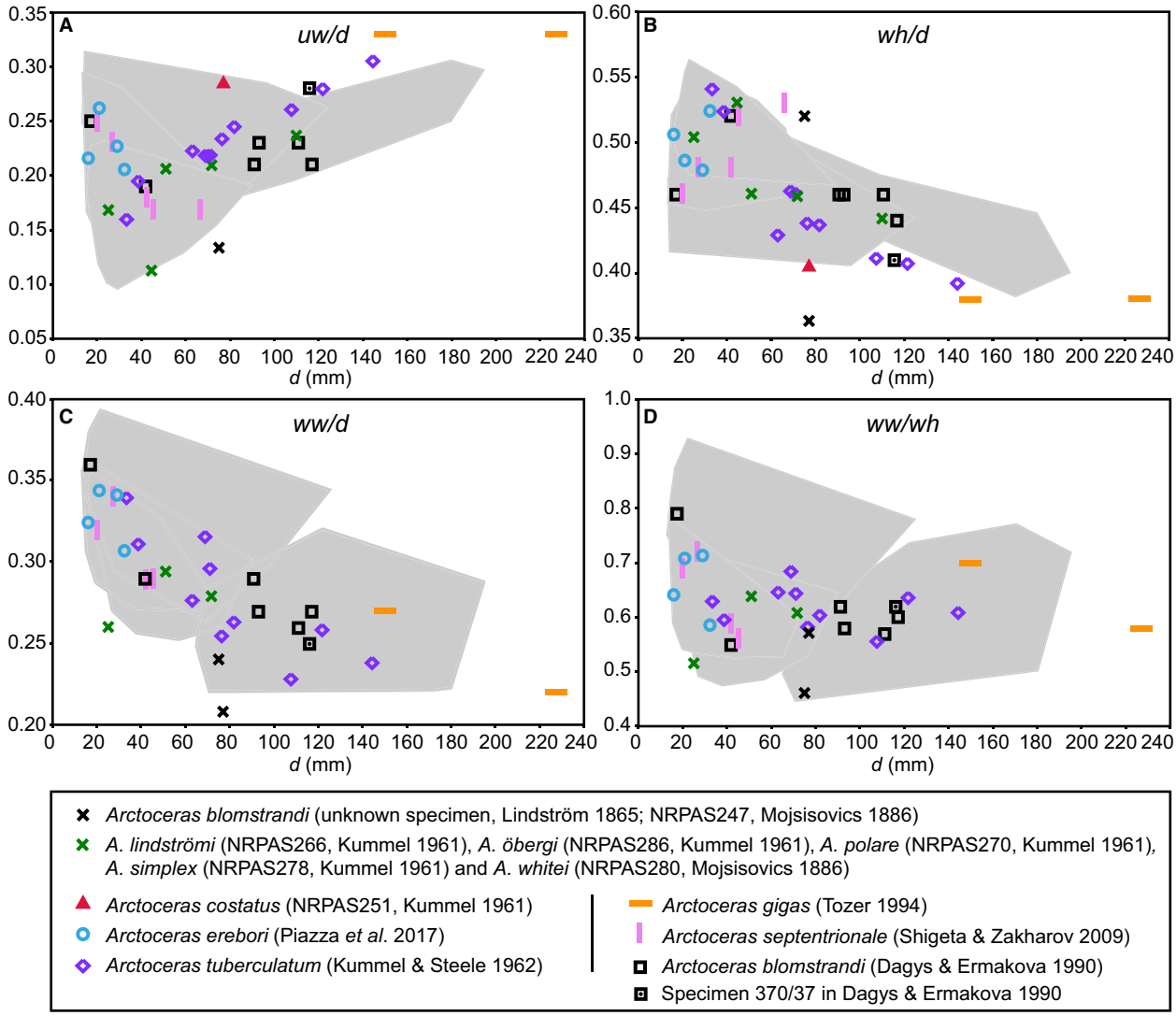

FIG. 11. Scatterplots comparing *Arctoceras* species in the literature (see legend) with *Arctoceras blomstrandi* of this study (grey polygons). A, umbilical width index *uw/d*. B, whorl height index *wh/d*. C, conch width index *ww/d*. D, whorl width index *ww/wh*. The Russian *Arctoceras blomstrandi* specimen 370/37 (Dagys & Ermakova 1990) is indicated with a dot in the black square and is discussed in the text. *Abbreviation*: NRPAS, Naturhistoriska Riksmuseet Paleozoologi Avdelning, Stockholm, Sweden.

top of the section did in fact grow to sizes similar to those seen in the bottom of the section. Only one fragmental specimen from −3.1 m might be used in direct support of this assumption: specimen PIMUZ37607 (Fig. 6F), which is the largest known individual from Group IV, with a diameter of 124.7 mm. It has *costatus*-like straight ribbing on an inner part of the conch and more 'classic' sigmoidal ribbing closer to the aperture. This could be interpreted as the retaining of the fully mature ornamentation at large sizes across the stratigraphy. However, the general absence of very large individuals (d > 130 mm) in most of the stratigraphy is difficult to explain if a constant mature size and ornamentation was maintained at all times. Preservation size biases would hardly be that consequent throughout that many metres of sediment. A possibility is, as mentioned above, that mature or near-mature individuals migrated to other areas. Finally, it is also a possibility that *A. blomstrandi* did actually evolve towards smaller mature sizes towards the top of the stratigraphy. It would be very interesting to see these possible answers studied in similar ways in other regions in the Boreal Realm.

Timing of the morphological change in Arctoceras blomstrandi

Much of the *Arctoceras blomstrandi* material is from the stratigraphic interval with $\delta^{13}C$ around −34‰. This

places them in the peak phase of the middle Smithian negative carbon isotope excursion (Hammer *et al.* 2019) that is associated with a spore spike and an ecological crisis of land plants (Hochuli *et al.* 2016) during the middle Smithian thermal maximum (Romano *et al.* 2013). The morphological changes in *A. blomstrandi* that give rise to *A. blomstrandi* var. *costatus* are seen to be initiated at *c.* −5 m in relation to the top of the Lusitaniadalen Member (and *c.* 2.6 m below our inferred base of the *W. tardus* Zone; Fig. 2). Thus, the initial change in *Arctoceras* morphology coincides with the initial increase in $\delta^{13}C$ in the uppermost middle Smithian, leading up to the major positive shift across the Smithian–Spathian boundary (Hammer *et al.* 2019). As mentioned above, *A. blomstrandi* might in fact be subject to miniaturization in the upper 5 m of the stratigraphy, which is not an uncommon response to environmental stresses (Urbanek 1993), and could very well be a likely explanation for the stratigraphic evolution observed in *A. blomstrandi*. However, we have not been able to assess the maturity of the present material, and it is not currently possible to test for an evolutionary change towards smaller conchs (miniaturization).

Comparisons with Arctoceras *observations in Arctic Canada and Siberia*

In 1994, Tozer described *A. blomstrandi* from several Smithian localities in Canada (Ellesmere and Axel Heiberg Islands, British Columbia and Alberta) and noted how they often have prominent umbilical tubercles. Rare specimens were, however, strikingly different. Tozer illustrated a specimen (GSC28154; Geological Survey of Canada) from Svartefjeld Peninsula that he assigned to *A. blomstrandi* (following Kummel 1961), but which he described as looking like *A. lindstroemi* (Mojsisovics) or *A. costatum* [*A. costatus*] (Öberg). Where other specimens from the same section bear weak ribs and distinct tubercles, GSC28154 bears strong ribs and only barely perceptible tubercles. Furthermore, the specimen was found in possible association with late Smithian taxa, and Tozer tentatively placed it in the *W. tardus* Zone (Tozer 1994, p. 74, pl. 27, fig. 1). Based on the given illustration (diameter appears to be no more than 90 mm), GSC28154 does indeed resemble *A. blomstrandi* var. *costatus*. The placement of GSC28154 in the *W. tardus* Zone is questionable and is probably due to severe condensation. In that case, GSC28154 can be expected to originate from the very top of the *Euflemingites romunderi* Zone, which gives it the same approximate age as *A. blomstrandi* var. *costatus* in Svalbard. The morphological evolution observed in *A. blomstrandi* in Svalbard would appear to be present also in Arctic Canada, and is hence useful in biostratigraphy in the Boreal Realm.

From Arctic Canada, Tozer (1994) also described the possibly late Smithian species *Arctoceras gigas* from the Blind Fiord Formation (*W. tardus* Zone?) at Lindström Creek, Ellesmere Island. *Arctoceras gigas* is defined as having sometimes dense tubercles, an inclined umbilical wall and a wider umbilicus than *A. blomstrandi* (Fig. 11A). Where *A. blomstrandi* has an umbilical width of less than 30% of the diameter (often *c.* 25%) *A. gigas* has an umbilical width of more than 30% (Tozer 1994). We find this to be in general accordance with our data, in which only three specimens have umbilical width indexes of more than 0.29. It is interesting to note that although two of these are large individuals from the bottom of the section, one is from the upper part at −3.1 m (horizon STA3) and is certainly a juvenile (d = 14.34 mm). The taxonomic relationship between *A. gigas* and *A. blomstrandi* would be highly interesting to see examined, given that *A. blomstrandi* is now shown to evolve towards a wider relative umbilicus. Tozer (1994) did not illustrate the suture line of *A. gigas* for our direct comparison to other *Arctoceras* species.

Dagys & Ermakova (1990) reported observations (in Russian) of *Arctoceras blomstrandi* from the *Kolymensis* Zone (= middle Smithian) of Siberia. The illustrated *Arctoceras* specimens with corresponding description and measurements fit well within the trends seen in Svalbard. The one suture line (Dagys & Ermakova 1990, fig. 18A) is of the more denticulate type, but still within the variation expected in *A. blomstrandi* (Fig. 4H–K). According to Dagys & Ermakova (1990), *A. blomstrandi* has a limited conch variability in Siberia (*uw/d*, 0.19–0.28; *wh/d*, 0.41–0.52; *ww/d*, 0.25–0.36; *ww/wh*, 0.55–0.79), and the major intraspecific variation arises from differences in the strength of ornamentation. Measurements of only five Russian specimens have been reported, and it is very possible that the authors did not sample the full range of conch variation in Siberian *A. blomstrandi*. The five Siberian specimens are fairly large and plot with Group I (and partly with Group IV) from Svalbard (Fig. 11). One Siberian specimen (372/37, d = 91 mm) was measured at three growth stages. The youngest stage (d = 17.4 mm) plots in the areas where Groups III and IV overlap, while the middle growth stage (d = 42 mm) plots with Groups II and III (Fig. 11). The three consecutive measurements of specimen 372/37 point to a very plastic development of the relative width of the umbilicus and the whorl. However, the specimen appears highly weathered from the illustration (Dagys & Ermakova 1990, pl. 9 fig. 2), and the measurements are considered with some caution here. Another specimen, 370/37 (Dagys & Ermakova 1990, pl. 9 fig. 2), bears straight ribs reminiscent of those of *A. blomstrandi* var. *costatus*, but also bears umbilical tubercles. The specimen has a much slimmer conch than specimens of Group IV (370/37 is marked with a dot in

Fig. 11), and is morphologically related to the large specimens of Group I. As at the time of writing, the *A. blomstrandi* var. *costatus* morphotype is unconfirmed in Siberia, and it is not currently possible to say if the morphological trends from Svalbard may be observed in Siberia.

CONCLUSION

It is a general issue in ammonoid palaeontology that long- and wide-ranging genera need improved definitions of conch morphology variability between, and within, species. A well-understood specific variation across stratigraphy would be beneficial to the biostratigraphical resolution and is something worth attempting within each basin. The middle Smithian *Arctoceras blomstrandi* was initially split into seven species (*A. blomstrandi*, *A. costatus*, *A. lindströmi*, *A. öbergi*, *A. polare*, *A. simplex* and *A. whitei*) in the late 1800s, only to be reformed as a single species by Kummel in 1961. However, the variation in conch morphology and ornamentation observed in the field appears to fall in stratigraphically distinct groups, and a revision of Svalbard *Arctoceras* was needed. For this study, we have collected new and extensive *Arctoceras* specimens from Svalbard within the Boreal Realm. Sections on Stensiöfjellet and Wallenbergfjellet in Sassendalen were logged and sampled to obtain material with a high degree of stratigraphic control. Several stratigraphic horizons yielded five or fewer specimens, and the horizons were sorted into four stratigraphic groups to enable meaningful analysis. We find that the variability in the investigated specimens does not exceed normal intraspecific variation. The variation is, however, not random, as proposed by Kummel (1961), but depends on stratigraphic position. A bias in recovered conch sizes between different parts of the section complicated the morphological analysis, but the ontogenetic development was shown to vary between the stratigraphic groups. In the major part of the *A. blomstrandi* species range, conch morphology and ornamentation follow the same ontogenetic trends. The observed variation is to a large degree controlled by the different developmental stages of the individual specimens. Towards the top of the species range, a shift in the conch morphology takes place, and the relative expansion of the umbilicus changes from allometric to isometric. At the same time, the whorl width is seen to increase slightly, and the whorl width index reaches larger values in the top than in any other part of the section. Ornamentation in the form of ribbing (coupled to conch morphology through Buckman's law of covariation) becomes stronger in the top, while umbilical tubercles are apparently not more common than earlier. The morphological shift in *A. blomstrandi* is located *c.* 5 m below the Smithian–Spathian boundary, and possibly 2.6 m below the middle–late Smithian boundary. A morphotype similar to the synonymized species *A. costatus* of Öberg (1877) is hence observed only in the uppermost part of the stratigraphy (3.6–2.1 m below the Smithian–Spathian boundary), and is considered as a morphological and stratigraphic endmember within the *A. blomstrandi* complex. The documented morphological trends in Spitsbergen provide a first reference study for forthcoming comparisons with occurrences from other latitudes. Such studies will ultimately contribute to disentangling evolutionary from ecological responses of ammonoids during the middle Smithian thermal maximum, i.e. the warmest climatic episode throughout the entire Early Triassic.

SYSTEMATIC PALAEONTOLOGY

By Bitten Bolvig Hansen

Order AMMONOIDEA Zittel, 1884
Family ARCTOCERATIDAE Arthaber, 1911

Genus ARCTOCERAS Hyatt, 1900

Type species. Ceratites polaris Mojsisovics, 1886; from central Spitsbergen in Svalbard, Norway.

Remarks. Seven species of *Arctoceras* described from Svalbard in the nineteenth century were lumped into the senior species *A. blomstrandi* (Lindström, 1865) by Kummel (1961). The one species of *Arctoceras* in Svalbard remains valid, but rare material assigned to the synonym species *C. costatus* (Öberg, 1877) is acknowledged as a distinct endmember morphology with a limited stratigraphic range, and is termed *A. blomstrandi* var. *costatus* (Öberg 1877, pl. 4, fig. 3).

Arctoceras blomstrandi (Lindström, 1865)
Figures 3–6

1865 *Ceratites? blomstrandi* Lindström, p. 4, pl. 1, fig. 3 [–5?].
1877 *Ceratites blomstrandi* Lindström; Öberg, p. 11, pl. 3, figs 1–4.
1877 *Ceratites costatus* Öberg, pp. 13–14, pl. 4, fig. 3–4.
1886 *Ceratites öbergi* Mojsisovics, pp. 33–34, pl. 7, figs 5–6, pl. 8. figs 1, 3.
1886 *Ceratites lindströmi* Mojsisovics, p. 35, pl. 8., fig. 2.
1886 *Ceratites simplex* Mojsisovics, pp. 30–31, pl. 6, figs 2–4.
1886 *Ceratites polaris* Mojsisovics, pp. 31–32, pl. 7, figs 1–2.
1886 *Ceratites* indet. Mojsisovics, p. 32, pl. 6, fig 7.

1886 *Ceratites whitei* Mojsisovics, pp. 32–33, pl. 6, figs 5–6.
1915 *Arctoceras blomstrandi* Lindström; Diener, p. 52.
1915 *Arctoceras costatus* Öberg; Diener, p. 52.
1915 *Arctoceras oebergi* Mojsisovics; Diener, p. 52.
1915 *Arctoceras lindströmi* Mojsisovics; Diener, p. 52.
1915 *Arctoceras simplex* Mojsisovics; Diener, p. 52.
1915 *Arctoceras polare* Mojsisovics; Diener, p. 52.
1915 *Arctoceras* sp. indet. Mojsisovics; Diener, p. 53.
1915 *Arctoceras whitei* Mojsisovics; Diener, p. 53.
1961 *Arctoceras oebergi* Mojsisovics; Tozer, pp. 68–69, pl. 15, figs 1–5, pl. 16, figs 2–4.
1978 *Arctoceras blomstrandi* Lindström; Weitschat & Lehmann, p. 85–100, pl. 12, fig. 1A–B.
1990 *Arctoceras blomstrandi* Lindström; Dagys & Ermakova, p. 40–43, pl. 9, figs 1–2, pl. 10, figs 1–2.
1994 *Arctoceras blomstrandi* Lindström; Tozer, pp. 74–75, pl. 26, figs 1–3, pl. 27, fig. 1.
2017 *Arctoceras erebori* Piazza *et al.*, p. 114–115, fig. 6E–I.

Emended diagnosis. Discoidal conch of moderate to sometimes strong compression. Conch is most commonly subinvolute, but small individuals ($d <$ ~70 mm) may be involute, and very rare individuals of various sizes can be subevolute. Flanks are subparallel to slightly convex, grading imperceptibly onto the venter. The whorl section is oval and widest at about mid-flank. The venter is narrowly to broadly rounded. Umbilical shoulder is angular and the umbilical wall vertical. Ornamentation consists most often of simple ribs, sometimes weak umbilical tubercles and rarely ventral strigation. The ribs are sinuous to straight, arranged distantly with a radial to prorsiradiate orientation. The ornamentation is variable across the species with some small to medium individuals lacking all sculpture, but ribs typically grow stronger through ontogeny. As a rule ribs are strong on large individuals ($d >$ ~100 mm), and umbilical tubercles are not seen on small individuals. Suture line is ceratitic with broad saddles and lobes bearing few lobules (2–4 in immature specimens and max. 6–7 in large mature specimens) (Fig. 4H–K).

In the top few (~2.6) metres of the *Arctoceras blomstrandi* stratigraphic range, the species tends towards relatively wider whorl sections and more evolute conchs compared with the rest of the range. Within this interval, the rare *A. blomstrandi* var. *costatus* may be observed. The morphotype bears prominent ribs that tend to be straight and may cross the venter. The umbilical shoulder can be somewhat rounded and there are no true umbilical tubercules, although the umbilical shoulder can be slightly raised. Whorl section becomes almost rectangular.

New material. 135 measured specimens collected from Stensiöfjellet and Wallenbergfjellet in Sassendalen, central Spitsbergen, Svalbard. 24 specimens are illustrated herein (PIMUZ37592–37604 and PIMUZ37606–37616), along with four suture lines (PIMUZ37593, PIMUZ37596, PIMUZ37600, PIMUZ37616).

Remarks. Arctoceras erebori from possibly the upper Smithian of Svalbard (Piazza *et al.* 2017) is indistinguishable from juveniles of *A. blomstrandi* both in ornamentation and in conch morphology (Fig. 11). *Arctoceras erebori* is described as having ventral strigation and sometimes a keel. Ventral strigation is not unknown in *A. blomstrandi*, and Lindström (1865) included the feature in the original description of *C. blomstrandi*. Examples of (very weak) ventral strigation are seen in PIMUZ37616 (Fig. 6C) and PIMUZ37592 (Fig. 6E). The proposed keel in *A. erebori* is present in only one specimen (PMO210.489) on a part of the venter that is collapsed, and the feature is here considered a preservation artefact. The suture line of *A. erebori* is of the more denticulate type, but not exceeding the variation otherwise seen in *A. blomstrandi*. The precise stratigraphic level of *A. erebori* is unknown, but according to museum notes, the material was found within a concretion in association with taxa typical of the *W. tardus* Zone. This association could not be confirmed from any of our bedrock-controlled collections. The association of *Arctoceras* with the *W. tardus* Zone is likely to be the result of local compaction or even reworking, and *A. erebori* is here considered a junior synonym of *A. blomstrandi*.

Arctoceras tuberculatum (Smith, 1932) from the early and middle Smithian of USA (Nevada, Kummel & Steele 1962; Jattiot *et al.* 2017; Jenks & Brayard 2018; California, Kummel & Steele 1962; Utah, Brayard *et al.* 2013) has a conch morphology very similar to that of *A. blomstrandi* as demonstrated in Figure 11. However, the umbilical shoulder of *A. tuberculatum* tends to be raised and to bear stronger tuberculation than is seen in any *A. blomstrandi* specimens. The suture line may be helpful in distinguishing between the two species, given that the lateral lobe is more dentate in *A. tuberculatum* than in *A. blomstrandi* in specimens of similar size.

Arctoceras rubyae (Jenks & Brayard, 2018) from the late early Smithian and early middle Smithian of Nevada has ornamentation and an umbilical width index comparable to that of *A. blomstrandi*, but the species is recognized from its extremely compressed conch (*ww/d*, 0.20–0.22).

Arctoceras gigas (Tozer, 1994) from the late middle Smithian or possibly the early late Smithian of Ellesmere Island (Arctic Canada) has a very similar appearance to *A. blomstrandi*. *Arctoceras gigas* is represented only by few and poorly preserved specimens, but is defined as being larger than *A. blomstrandi*, as well as having a wider umbilicus (*uw/d* <0.30) with denser umbilical tubercles. *Arctoceras gigas* is indeed very large, but the specimens measured by Tozer (1994) seem to share ontogentic trends with both *A. blomstrandi* and *A. tuberculatum* (as suggested by Brayard *et al.* 2013) (Fig. 11). More material with suture lines preserved would be needed to either confirm the species *A. gigas* or to treat it as a synonym of another *Arctoceras* species.

Arctoceras strigatus from Guangxi (South China) (Brayard & Bucher 2008) has a very weak radial ornamentation and profound strigation, setting it apart from *A. blomstrandi*. The suture line is also more dentate in *A. strigatus*.

Arctoceras septentrionale (Diener, 1895) and *A. subhydapsis* (Kiparisova, 1961) from the Smithian of South Primorye (Russia) as described by Shigeta & Zakharov (2009), are difficult to confirm as separate species, because they might as well represent different maturity stages. *Arctoceras septentrionale* is not truly

distinguishable from juvenile *A. blomstrandi* in either ornamentation or conch morphology (Fig. 11). *Arctoceras subhydapsis* is more evolute and has a more dentate suture line than *A. blomstrandi*, but more material of the two Russian species would be useful before a confident conclusion can be made on the taxonomy.

Arctoceras schalteggeri from the early Smithian of Pakistan (Brühwiler *et al.* 2011) has a conch morphology similar to that of *A. blomstrandi*, but ornamentation is simpler and weaker, and the suture line appears to be more denticulate.

Occurrence. *Arctoceras blomstrandi* is common in middle Smithian sections throughout central Spitsbergen, Svalbard. *Arctoceras blomstrandi* var. *costatus* is found only within the upper few (~2.6?) metres of the range. *Arctoceras blomstrandi* is also found in localities in Canada (Ellesmere and Axel Heiberg Islands, British Columbia and Alberta) (Tozer 1961, 1994) and Siberia (Dagys & Ermakova 1990), and possibly at Crittenden Springs, Nevada (HB, pers. obs.)

Acknowledgements. We would like to extend our heartfelt thanks to Franz-Josef Lindemann (NHM) for his thorough fieldwork preparations and assistance in the field. Rosi Roth (UZH) is thanked for her major assistance in preparation and specimen photography, while Markus Hebeisen (UZH) is thanked for making equipment available and for his guidance in preparation. HB thanks the Swiss NSF for its support (projects 160055 and 180253). Yuri D. Zakharov and an anonymous referee commented on an earlier draft of this manuscript and are thanked for the major improvements to the final version.

DATA ARCHIVING STATEMENT

Data for this study are available in the Dryad Digital Repository: https://doi.org/10.5061/dryad.vq83bk3qw

Editor. Arnaud Brayard

REFERENCES

BRAYARD, A. and BUCHER, H. 2008. Smithian (Early Triassic) ammonoid faunas from northwestern Guangxi (South China): taxonomy and biochronology. *Fossils & Strata*, **55**, 1–179.

—— —— 2015. Permian–Triassic extinctions and rediversifications. 465–473. *In* KLUG, C., KORN, D., DE BAETS, K., KRUTA, I. and MAPES, R. (eds) *Ammonoid paleobiology: From macroevolution to paleogeography*. Topics in Geobiology, **44**. Springer, 615 pp.

—— —— ESCARGUEL, G., FLUTEAU, F., BOURQUIN, S. and GALFETTI, T. 2006. The Early Triassic ammonoid recovery: paleoclimatic significance of diversity gradients. *Palaeogeography, Palaeoclimatology, Palaeoecology*, **239**, 374–395.

—— BYLUND, K. G., JENKS, J. F., STEPHEN, D. A., OLIVIER, N., ESCARGUEL, G., FARA, E. and VENNIN, E. 2013. Smithian ammonoid faunas from Utah: implications for Early Triassic biostratigraphy, correlation and basinal paleogeography. *Swiss Journal of Palaeontology*, **132**, 141–219.

BRÜHWILER, T., BUCHER, H., BRAYARD, A. and GOUDEMAND, N. 2010. High-resolution biochronology and diversity dynamics of the Early Triassic ammonoid recovery: the Smithian faunas of the Northern Indian Margin. *Palaeogeography, Palaeoclimatology, Palaeoecology*, **297**, 491–501.

—— —— ROOHI, G., YASEEN, A. and REHMAN, K. 2011. A new early Smithian ammonoid fauna from the Salt Range (Pakistan). *Swiss Journal of Palaeontology*, **130**, 187–201.

BUCHAN, S. H., CHALLINOR, A., HARLAND, W. B. and PARKER, J. R. 1965. The Triassic stratigraphy of Svalbard. *Norsk Polarinstitutt Skrifter*, **135**, 1–97.

BUCKMAN, S. S. 1892. *A monograph of the ammonites of the Inferior Oolite Series*. Palaeontographical Society, London, 456 p.

DAGYS, A. S. 1994. Lower Triassic stage, substage and zonal scheme of north-eastern Asia. 15–22. *In* GEUX, J. and BAUD, A. (eds) *Recent developments on Triassic stratigraphy*. Mémoires de geologie (Lausanne), **22**, 192 pp.

—— and ERMAKOVA, S. P. 1990. *Early Olenekian ammonoids of Siberia*. Nauka, Moscow, 112 pp. [In Russian]

DE QUEIROZ, K. 1998. The general lineage concept of species, species criteria, and the process of speciation. 57–75. *In* HOWARD, D. J. and BERLOCHER, S. H. (eds) *Endless forms: Species and speciation*. Oxford University Press, 470 pp.

DIENER, C. 1915. *Fossilium Catalogus I, Animalia: pt. 8 Cephalopoda Triadica*. W. Junk, Berlin, 369 pp.

FREBOLD, H. 1930. Die alterstellung des fischhorizontes, des grippianiveaus and des unteren saurierhorizontes in Spitzbergen. *Skrifter om Svalbard og Ishavet*, **28**, 52.

GALFETTI, T., HOCHULI, P. A., BRAYARD, A., BUCHER, H., WEISSERT, H. and VIGRAN, J. O. 2007. Smithian-Spathian boundary event: evidence for global climatic change in the wake of the end-Permian biotic crisis. *Geology*, **35**, 291–294.

GOUDEMAND, N., ROMANO, C., LEU, M., BUCHER, H., TROTTER, J. and WILLIAMS, I. 2019. Dynamic interplay between climate and marine biodiversity upheavals during the Early Triassic Smithian–Spathian biotic crisis. *Earth-Science Reviews*, **95**, 169–178.

HAMMER, Ø. and BUCHER, H. 2005. Buckman's first law of covariation: a case of proportionality. *Lethaia*, **38**, 67–72.

—— HARPER, D. A. T. and RYAN, P. D. 2001. Past: paleontological statistics software package for education and data analysis. *Palaeontologia Electronica*, **4** (1), 9.

—— JONES, M., SCHNEEBELI-HERMANN, E., HANSEN, B. B. and BUCHER, H. 2019. Are Early Triassic extinction events associated with mercury anomalies? A reassessment of the Smithian/Spathian boundary extinction. *Earth-Science Reviews*, **195**, 179–190.

HANSEN, B. B., BUCHER, H., SCHNEEBELI-HERMANN, E. and HAMMER, Ø. 2020. Data from: The middle Smithian (Early Triassic) ammonoid *Arctoceras blomstrandi*: conch morphology and ornamentation in relation to stratigraphy. *Dryad Digital Repository*. https://doi.org/10.5061/dryad.vq83bk3qw

HOCHULI, P. A., SANSON-BARRERA, A., SCHNEEBELI-HERMANN, E. and BUCHER, H. 2016. Severest crisis overlooked: worst disruption of terrestrial environments postdates the Permian–Triassic mass extinction. *Scientific Reports*, **6**, 7.

JATTIOT, R., BUCHER, H., BRAYARD, A., MONNET, C., JENKS, J. F. and HAUTMANN, M. 2016. Revision of the genus *Anasibirites* Mojsisovics (ammonoidea): an iconic and cosmopolitan taxon of the late Smithian (Early Triassic) extinction. *Papers in Palaeontology*, **2**, 155–188.

—— —— —— BOSSE, M., JENKS, J. F. and BYLUND, K. G. 2017. Smithian ammonoid faunas from northeastern Nevada: implications for Early Triassic biostratigraphy and correlation within the western USA basin. *Palaeontographica Abteilung A*, **309**, 1–89.

JENKS, J. F. and BRAYARD, A. 2018. Smithian (Early Triassic) ammonoids from Crittenden Springs, Elko County, Nevada: taxonomy, biostratigraphy and biogeography. *New Mexico Museum of Natural History & Science Bulletin*, **78**, 1–175.

KLUG, C., KORN, D., LANDMAN, N. H., TANABE, K., DE BAETS, K. and NAGLIK, C. 2015. Describing ammonoid conchs. 3–24. *In* KLUG, C., KORN, D., DE BAETS, K., KRUTA, I. and MAPES, R. H. (eds) *Ammonoid paleobiology: From anatomy to ecology*. Topics in Geobiology, **43**, 934 pp.

KORCHINSKAYA, M. V. 1972. Biostratigraphy of Triassic deposits of Svalbard. *Bulletin of Canadian Petroleum Geology*, **20**, 742–749.

KUMMEL, B. 1961. The Spitsbergen Arctoceratids. *Bulletin of the Museum of Comparative Zoology at Harvard College*, **123**, 499–532, figs 1–5, pl. 1–9.

—— and STEELE, G. 1962. Ammonites from the Meekoceras gracilitatus Zone at Crittenden Spring, Elko County, Nevada. *Journal of Paleontology*, **36**, 638–703.

LINDSTRÖM, G. 1865. Om Trias- och Juraförsteningar från Spetsbergen. *Kongliga Svenska Vetenskapsakademiens Handlingar*, **6**(6), 1–20.

MAJOR, H., HAREMO, P., DALLMANN, W. K. and ANDRESEN, A. 2001. Geological Map of Svalbard 1:100,000 Sheet C9G Adventdalen. Norwegian Polar Institute. www.npolar.no

MOJSISOVICS VON MOJSVÁR, E. 1886. Arktische Triasfaunen. *Mémoires de L'Académie Impériale des Sciences St. Petersbourg, Serie 7*, **33(6)**, 1–159, pl. 1–20.

MONNET, C., DE BAETS, K. and YACCOBUCCI, M. M. 2015. Buckman's rules of covariation. 67–94. *In* KLUG, C., KORN, D., DE BAETS, K., KRUTA, I. and MAPES, R. (eds) *Ammonoid paleobiology: From macroevolution to paleogeography*. Topics in Geobiology, **44**. Springer, 615 pp.

MØRK, A., ELVEBAKK, G., FORSBERG, A. W., HOUNSLOW, M. W., NAKREM, H. A., VIGRAN, J. O. and WEITSCHAT, W. 1999. The type section of the Vikinghøgda Formation: a new Lower Triassic unit in central and eastern Svalbard. *Polar Research*, **18**, 51–82.

MOULTON, D. E., CHIRAT, R. and GORIELY, A. 2015. The morpho-mechanical basis of ammonite form. *Journal of Theoretical Biology*, **364**, 220–230.

NORWEGIAN POLAR INSTITUTE 2003. *The place names of Svalbard*. Rapportserie nr. 122, Norwegian Polar Institute, Polar Environmental Centre, Tromsø, 537 pp.

ÖBERG, P. 1877. Om Trias-försteningar från Spetsbergen. *Kongliga Svenska Vetenskapsakademiens Handlingar*, **14**, 1–19, pl. 1–5.

PIAZZA, V., HAMMER, Ø. and JATTIOT, R. 2017. New late Smithian (Early Triassic) ammonoids from the Lusitaniadalen Member, Vikinghøgda Formation, Svalbard. *Norwegian Journal of Geology*, **97**, 105–117.

ROMANO, C., GOUDEMAND, N., VENNEMANN, T. W., WARE, D., SCHNEEBELI-HERMANN, E., HOCHULI, P. A., BRÜHWILER, T., BRINKMANN, W. and BUCHER, B. 2013. Climatic and biotic upheavals following the end-Permian mass extinction. *Nature Geosciences*, **6**, 57–60.

SHIGETA, Y. and ZAKHAROV, Y. D. 2009. Systematic palaeontology: cephalopods. 44–140. *In* SHIGETA, Y., ZAKHAROV, Y. D., MAEDA, H. and POPOV, A. M. (eds) *The Lower Triassic system in the Abrek Bay area, South Primorye, Russia*. National Museum of Nature and Science, Tokyo, **38**, 224 pp.

TOZER, E. T. 1961. Triassic stratigraphy and faunas, Queen Elizabeth Islands, Arctic Archipelago. *Geological Survey of Canada Memoir*, **316**, 195.

—— 1994. Canadian Triassic ammonoid faunas. *Geological Survey of Canada Bulletin*, **467**, 667.

TYSON, R. V. 1995. *Sedimentary organic matter: Organic facies and palynofacies*. Chapman & Hall, 590 pp.

URBANEK, A. 1993. Biotic crises in the history of Upper Silurian graptoloids: a palaeobiological model. *Historical Biology*, **7**, 29–50.

WARE, D., BUCHER, H., BRAYARD, A., SCHNEEBELI-HERMANN, E. and BRÜHWILER, T. 2015. High-resolution biochronology and diversity dynamics of the Early Triassic ammonoid recovery: the Dienerian faunas of the Northern Indian Margin. *Palaeogeography, Palaeoclimatology, Palaeoecology*, **440**, 363–373.

WEITSCHAT, W. and DAGYS, A. S. 1989. Triassic biostratigraphy of Svalbard and a comparison with NE-Siberia. *Mitteilungen aus dem Geologisch-Paläontologischen Institut der Universität Hamburg*, **68**, 179–213.

—— and LEHMANN, U. 1978. Biostratigraphy of the uppermost part of the Smithian Stage (Lower Triassic) at the Botneheia, W-Sptsbergen. *Mitteilungen aus dem Geologisch-Paläontologischen Institut der Universität Hamburg*, **48**, 85–100.

WESTERMANN, G. E. G. 1966. Covariation and taxonomy of the Jurassic ammonite *Sonninia adicra* (Waagen). *Neues Jahrbuch für Geologie und Paläontologie, Abhandlungen*, **124**, 289–312.

WIDMANN, P., BUCHER, H., LEU, M., VENNEMANN, T., BAGHERPOUR, B., SCHNEEBELI-HERMANN, E., GOUDEMAND, N. and SCHALTEGGER, U. 2020. Dynamics of the largest carbon isotope excursion during the Early Triassic biotic recovery. *Frontiers in Earth Science*, **8**, 1–16 (article 196).

WIGNALL, P., BOND, D. P. G., SUN, Y., GRASBY, S., BEAUCHAMP, B., JOACHIMSKI, M. and BLOMEIER, D. 2016. Ultra-shallow-marine anoxia in an Early Triassic shallow-marine clastic ramp (Spitsbergen) and the suppression of benthic radiation. *Geological Magazine*, **153**, 316–331.